DEVELOPMENT AND CHARACTERIZATION OF A STOPPED-FLOW-BYPASS ANALYSIS SYSTEM WITH APPLICATIONS TO BIOCHEMICAL MEASUREMENTS

by
Stephen Wayne Hillard

Dissertation submitted to the Faculty of
Virginia Polytechnic Institute and State University
in partial fulfillment of the requirements for the degree of

DOCTOR OF PHILOSOPHY
in
Biochemistry

Committee:
Kent K. Stewart, Chairman
David R. Bevan
George E. Bunce
Thomas W. Keenan
Harold M. McNair

Keywords: **Analytical Instrumentation, Flow Injection Analysis, Assay Automation, Enzyme Assays, Genetic Transcription Assay, Stopped Flow, Physical Steady State**

March 1997
Blacksburg, Virginia

DEVELOPMENT AND CHARACTERIZATION OF A STOPPED-FLOW-BYPASS ANALYSIS SYSTEM WITH APPLICATIONS TO BIOCHEMICAL MEASUREMENTS

by
Stephen Wayne Hillard

Kent K. Stewart, Chairman
Department of Biochemistry

(ABSTRACT)

A new apparatus called Bypass Trapped Flow Analysis System (ByT-FAS) is described. A properly designed ByT-FAS gives an analyst the ability to use analyte sample volumes of 10 to 200 µL [or more] and reagent volumes of approximately the same size. The sample and reagent are injected into their respective carrier streams and attain physical steady state concentrations in the detection cell within approximately 15 to 45 seconds after injection. Upon achievement of simultaneous sample and reagent physical steady state concentrations, the system flow is diverted around the detection cell and the reaction mixture is trapped in the detection cell. The concentration of the sample and reagent in the detection cell can be readily computed from knowledge of the original concentrations of the sample and reagent and the flow rates of the streams propelling the sample and reagent. ByT-FAS was demonstrated to be useful for direct measurements of analytes in liquid solutions and for assays which utilize equilibrium and/or kinetic methods to create measurable product(s) for ultraviolet/visible spectrophotometry, fluorimetry, and chemiluminescence. Enzyme activities and fundamental enzyme kinetic parameters (Kms, Kis, VMAXs) were determined directly. Genetic transcription levels of luciferase in whole intact *E. coli* cells were also determined using chemiluminescent detection. Flow system configuration, components, and flow ratios were investigated for their effects on achieving physical steady state signals in the detector. It is believed that this new type of instrumentation will be of significant use for the analytical chemical, biochemical, molecular biology, biotechnology, environmental, pharmaceutical and medical communities for those measurements which require direct knowledge of the concentration of the reactants and products during quantitation.

Acknowledgements

I would like to thank my advisor, Dr. Kent K. Stewart, for his guidance, support, and willingness to always talk with me. I would also like to thank the members of my committee, Dr. David Bevan, Dr. George E. Bunce, Dr. Thomas Keenan , and Dr. Harold McNair for their suggestions for the improvement of my research efforts.

I would like to thank my fellow graduate students and department faculty and staff for their friendship and assistance.

I would like to thank my parents for their love and encouragement during all of my educational years. Lastly, but certainly not least, I would like to thank my wife Katya, for her love, friendship and support.

Table of Contents

List of Figures

List of Tables

Abbreviations

3wv-0A	three way valve number 0, letter A
3wv-0B	three way valve number 0, letter B
3wv-1	three way valve number 1
ADP	adenosine 5' diphosphate
ATP	adenosine 5' triphosphate
AU	absorbance unit
BCA	bicinchoninic acid
BCG	brom-cresol green
BSA	bovine serum albumin
ByT-FAS	Bypass Trapped-Flow Analysis System
C	Celsius
cm	centimeter(s)
DC	detector cell
dL	deciliter(s)
EC	enzyme commission
EDTA	ethylenediamine tetra-acetic acid
FIA	Flow Injection Analysis
FITC-BSA	fluorescein isothiocyanate labeled bovine serum albumin
G6PDH	glucose-6-phosphate dehydrogenase
gm	gram(s)
i.d.	internal diameter
Ki	enzyme inhibition constant
Km	Michaelis constant
LB	Lennox broth
LOD	limit of detection
M	molar
mg	milligram(s)
min	minute(s)
mL	milliliter(s)
mm	millimeter(s)
mM	millimolar
MOPS	(3-[N-Morpholino]propanesulfonic acid)
N	Normal
$NADP^+$	oxidized nicotinamide adenine dinucleotide phosphate
NADPH	reduced nicotinamide adenine dinucleotide phosphate
ng	nanogram
nm	nanometer
nM	nanomolar

OD	outer diameter
ONPG	*ortho*-nitrophenyl galactoside
p-HPA	*para*-hydroxy phenylacetic acid
p-NPP	*para*-nitrophenylphosphate
PEEK	poly ether ether ketone
R^2	linear correlation coefficient
s	second(s)
S.D.	standard deviation
SDS	sodium dodecylsulfate
SFA	Segmented Flow Analysis
SIV(s)	sample (reagent) standard chromatography injection valve
T	T - intersection
TAA	Technicon AutoAnalyzer
t_b	time from baseline to baseline
U	enzyme units
*u*g	microgram(s)
*u*L	microliter(s)
*u*M	micromolar
umol	micromole
Vmax	maximum enzyme velocity

Introduction

Life science research has expanded dramatically in the last several decades. With this expansion has come the need for more sophisticated methods of analysis and an ever increasing need for improved cost efficiency per assay.[1-3] The quantity of samples analyzed annually using automated instrumentation is exceptionally large. Clinical chemistry laboratories alone assay several million samples.[4] This is placing extensive demands upon the analytical capabilities of scientists. However, existing automated and semi-automated instrumentation for the life sciences and biotechnology fulfill the needs in only a limited fashion.

Commercially available analytical instruments for assay automation meet the needs of researchers in a restricted fashion because they have limited advantages of application over manual assay systems. In other words, each instrument can perform an assay with only one or two significant advantages over manual techniques, and frequently any advantage gained is also accompanied by some disadvantages.

For example, nonsegmented continuous analyzers commonly known as flow injection analysis (FIA), has excellent sample throughput of 60-300 samples per hour, but they are compromised by poor limits of detection and limited linear ranges compared with manual methods due to dilution by laminar dispersion.[5-7] Conversely, segmented flow continuous analyzers (SFA), widely known by the commercial name Technicon AutoAnalyzer (TAA) are widely employed for automated analysis in clinical laboratories but are mechanically complex as a result of the air bubbles used to separate samples.[8]

Automatic batch analyzers, such as the centrifugal fast analyzers, were developed as a prototype at Oak Ridge National Laboratories under the sponsorship of the National Institute of General Medical Sciences and the U.S. Atomic Energy Commission.[9] Consequently, this type of fast analyzer is known as a GeMSAEC system. These instruments are semi-automated systems that preserve individual sample integrity by giving each its own reaction vessel. However, it is limited in its ability to perform kinetic assays (especially continuous kinetics) and has obligatory manual transfer steps of the sample disk to the centrifugal analyzer.[10] Nonetheless, the instrument does have the advantages of preserved sample integrity and parallel analysis of multiple samples simultaneously.

No existing automated instrument combines the attributes of small sample volumes, knowledge of absolute concentrations, semi-automation, and assay and detector flexibility all in one package. Consequently, there is an existing need for such a system.

The objective or goal of this research was to continue development of a new semi-automated assay instrument that combines more types of assays with a variety of detectors and performs direct measurements on small injected sample volumes. The potential users of this refined instrument could be; biochemists, molecular biologists, clinical chemists, pharmaceutical companies, medical doctors, food chemists, and analytical chemists.

Bypass **T**rapped - **F**low **A**nalysis **S**ystem **(ByT-FAS)** is a second generation FIA system conceptualized and designed in the late 1980s by Kent Stewart. A schematic diagram of the prototype instrument is shown in Figure 2.1 (p 19).

ByT-FAS is currently designed to enable the performance of semi-automated continuous flow analysis of wet chemistry assays using small sample volumes while circumventing the diluting affects of laminar dispersion. The initial system design required injected sample and reagent volumes of 200 *u*L each to attain physical steady state concentrations at the point of detection. The initial design of the instrument was demonstrated to be successful by Kent Stewart with a UV/VIS spectrophotometric detection cell.[11]

Instrumentation

Regarding improvements to the ByT-FAS instrument, initial research goals were to, 1) decrease the volumes of sample and reagent required to attain physical steady state, 2) investigate the potential of using other detection modes (fluorescence and chemiluminescence).

Assay Applications

With the initial ByT-FAS instrument design, the types of assays that were shown to be feasible included, direct concentration measurements of low and high molecular weight compounds (dinitrophenyl-glutamate, and hemoglobin respectively), equilibrium measurement protein assays (brom-cresol green), and kinetic measurement protein assays (bicinchoninic acid (BCA).[12] These assays were successful in accordance with the instrument's design. However, different assay systems were also needed to fully demonstrate ByT-FAS's applicability and flexibility.

ByT-FAS is believed to be the first small volume (<100 *u*L sample) continuous flow system with the capability for a portion of the injected sample and reagent boluses to attain physical steady state (dilution only with reagent or sample and not by laminar dispersion). As a result, it was postulated that ByT-FAS could, for the first time, offer a semi-automated continuous flow methodology for conducting enzymological experiments using physical steady state measurements (determinations of Km's, Vmax, kcat etc.).

In summary, the goal of this research with ByT-FAS can be broken down into two main objectives: 1) modification of ByT-FAS's system design to enhance its capabilities; 2) development of better methods for analysis of enzymes with ByT-FAS. The improvement of ByT-FAS technology through alteration of the instrument's physical components, based on experimental and literature evidence, has been successful. The potential implications of ByT-FAS to wet chemistry assays include less labor intensive assays, higher sample throughput via semi-automation, and reduction in volume and cost of toxic reagents and expensive samples. This research will serve to broaden the instrument base of non-segmented continuous flow systems (with new characteristics) and offer exciting new avenues of pursuit for instrument development and assay applications.

Background and Significance

Instrumentation

-Segmented Continuous Flow Analyzers

Research into the development and manufacturing of automated wet chemistry analyzers originated in the middle 1950's by the acknowledged pioneer of flowing stream instrument automation Leonard Skeggs.[8] Skeggs developed the first continuous flow system which employed air-

segmentation of injected samples to avoid dilution by laminar dispersion. This prototype design was eventually developed into a commercial instrument by the Technicon Corporation and is commonly known by the brand name Technicon AutoAnalyzer (TAA).

Segmented flow analyzers have become widely accepted and used, especially in clinical laboratories.[10] However, several factors that limit the flexibility and versatility of segmented analyzers include; a complex mechanism for the reproducible introduction and removal of air bubbles, air segmentation of samples inhibits miniaturization, and sample and reagent volumes are relatively large (0.5-2.0 mL).[10]

-Centrifugal Fast Analyzers

In the late 1960's, research into the development of discrete sample fast analyzers was documented in several papers by Norman G. Anderson.[9,13] With a GeMSAEC fast centrifugal analyzer, the batch of samples are analyzed simultaneously. The analyzer does this by placing the individual samples and reagent in separate cavities on a special centrifugal rotor. The rotor is then placed into a centrifuge where the sample and reagent are radially swept and mixed into a disposable cuvette for spectrophotometric analysis. As the individual cuvettes pass by a stationary light source, the absorbance of the individual samples can be measured.[9]

These types of analyzers also became commercially manufactured and competed directly with segmented flow analyzers in clinical chemistry laboratories. This instrument's main limitations are that it is not fully automatable because of the transfer of the sample disk to the centrifuge rotor and that it requires a significant capital investment.[10]

-Robotic Assay Analyzers

For analytical analysis laboratories that have a lot of time-consuming sample treatment and analysis steps, and have a high sampling frequency, robotic workstations offer the desired automation.[10] While the other types of automated instruments described above and below bring the reagent and sample together and measure products in a variety of ways, the robotic instrument can also perform tasks such as weighing, dispensing and transfer of liquids via microprocessor controlled syringes, assembling of tubes, beakers, shaking, sealing of vials, and heating.[10] The ability of robotics to replace essentially every step that an analyst can perform is initially intriguing. However, the cost of such systems is high; too high for all but the most robustly funded projects. However, technological development may someday bring costs of these analyzers down.[14]

-Non-FIA Traditional Stopped-Flow Systems

The traditional rapid expulsion-syringe stopped-flow systems have the advantages of rapid mixing, and the ability to make measurements on the order of a 0.01 second time scale with the first point being taken approximately 0.03 seconds after mixing.[15] These systems are used for the study of rapid kinetic reactions (<1 second). Based on the use of this instrument to evaluate kinetic data, the system flow and detection systems were designed such that the analyst could compute the absolute concentrations of any component of the reaction mixture. The traditional rapid expulsion-syringe stopped flow systems have the disadvantages that each assay requires large sample and

reagent volumes (about 2 ml each), and a poor sample through-put because the system has to be drained, and the syringes recharged between each assay.[14] The complexity of these systems does not enable them to be used for traditional multiple assays.

-Nonsegmented Continuous Flow Analysis (FIA)

FIA was simultaneously but independently developed in the mid 1970s by two research groups led by Kent K. Stewart and Jaromir Růžička.[5,6]

The concept of FIA is relatively simple and easy to understand. A sample is injected into a continuously flowing stream where it may mix with a reagent at an intersection, flow through a reaction coil to accumulate product, and ultimately flow into a detector for quantitative measurement. Many variations of the FIA manifold have been developed depending on the type of assay and/or detection method needed.[16]

FIA is a relatively mature field with at least six monographs on the subject published from 1981 to 1991.[4,10,16-20] There also exists an international journal solely dedicated to FIA research articles called the Journal of Flow Injection Analysis. Including all research journals, over 3,000 papers were published on FIA as of 1991.[17]

As evidenced by the literature base on FIA, the instrument has generated considerable interest in the field of assay automation. Even though FIA methodology does have the advantages of higher sample throughput and full automation, it has failed to gain the extent of commercialization and clinical laboratory acceptance of the other automated analyzers described above.

-FIA Measurement

An assay in which the concentrations of reactants at the point of detection is known is referred to as a direct-measurement or absolute concentration assay. Assays in which the concentrations of reactants are not known are referred to as relative measurements. FIA quantification of assay data has almost always relied upon relative measurements because of the diluting effects of laminar dispersion (described below). Because FIA does not achieve physical steady state as it is traditionally used, it cannot be used for assays that require direct measurements.

-Laminar Dispersion

In all pressure pumped flowing stream systems (peristaltic, syringe, air pressure, reciprocating, etc.) except electroosmotic flow, there is a phenomenon called laminar flow. The persistent and deleterious consequences of this phenomenon to sample integrity in a flowing stream served as the basis for air-segmentation by Skeggs.

The physical description of laminar flow is as follows. A flowing stream through cylindrical tubing has a differential velocity across the radius of the tubing, with the largest velocity occurring in the center. This differential flow velocity originates from the friction of the solution against the wall of the tubing. As the distance away from the tubing wall increases, the effect of friction from the wall on the solution decreases. As a result, a sample bolus injected into this stream would become dispersed into the shape of finely pointed spear at the front with a large conical cavity protruding into the back. Laminar flow is typically referred to in the FIA literature as laminar dispersion because of

its diluting affects to injected boluses. Flow profiles of sample boluses in FIA have been mathematically computed and diagrammed.[21] This dramatic diluting effect has been extensively researched by the FIA community to reduce its effects. Early descriptive models of sample dispersion in a flow stream like the tanks-in-a-series model were adapted by FIA researchers to explain dispersion of a sample zone in a carrier stream. The tanks-in-series model is based on the idea that an injected liquid flows through a series of well stirred tanks of equal size as has been described in textbooks of chemical reactor engineering.[22,23] This model has limited use and is not generally applicable to FIA. For example, the theory only applies to sample dispersion zones moving at a constant speed. Also, the injection of the sample and reagent, as well as the confluence of sample and reagent at mixing points, or stopped flow conditions are not treated with this theory.[22]

Physically more descriptive models of laminar dispersion had been developed by the chromatography research community like that put forth by Taylor in 1953 and 1954 for the solution of the diffusion-convection equation for dispersion in a flowing stream.[24,25] The solution of the diffusion-convection equation for the degree of dispersion (measured by the time for signal to go from baseline to baseline) occurring in a flowing stream was put forth by Vanderslice *et al* in 1981 using the method of solution of the equation given by Ananthakrishnan *et al*, 1965.[7,26] This theory accounts for the effects of chemical diffusion of the injected bolus. From this paper, the physical parameters of an FIA system that effect sample bolus dispersion (measured by the time from baseline to baseline) are given by the equation

$$t_b = 35.4\ a^2\ f\ (L/q)^{0.64}/\ D^{0.36} \qquad (1.1)$$

where a is the tubing radius, f is a proportionality constant, L is the tubing length, q is the flow rate, and D is the diffusion coefficient of the sample analyte. With the knowledge of the physical parameters of an FIA system that affect sample dispersion (namely tubing radius, length, and flow rate), ByT-FAS was designed in the late 1980's by Stewart to circumvent, not eliminate the diluting effects of laminar flow.

-FIA Design Variations

-FIA Stopped Flow Systems

Several FIA systems can have sample throughputs of up to 200 samples per hour. However, classic FIA assays have a lower sensitivity and poorer limit of detection than many manual and continuous flow analyzer assays. Two reasons for this lower sensitivity and poorer limit of detection are short reaction times in FIA systems (typically less than a minute) and the dilutions of the sample bolus due to laminar flow. Stopped flow FIA eliminates the loss of sensitivity due to short reaction times but does not deal with the dilutions of the sample bolus from laminar flow. Stopped flow FIA systems halt flow through the detector cell so a portion of the dispersed sample bolus is trapped to permit a longer reaction time. There are two different embodiments for systems that have been used to stop the flow in stopped flow FIA.

First, the flow through the entire system can be stopped by stopping the pump.[27] However, this technique can significantly reduce sample throughput because of the need for system flow pressures to reequilibrate after each sample detection.

Another technique to perform stopped flow FIA measurements is to divert the system flow around the detection cell during the desired measurement time.[28-30] This technique allows the pump to continue pumping and does not affect the overall system flow pressure as greatly as stopping the pump.

The diversion of system flow to achieve stopped flow FIA measurements has been accomplished in three different ways. First, a three way valve was placed between the point of injection and the detector cell. [28] Alternatively, a multiport injection valve was used to trap a portion of the injected sample in one of the loops between two of the injection ports.[29] Furthermore, another stopped flow FIA design used two multiport injection valves and trapped the injected sample and reagent between the two multiport injection valves.[30]

Regardless of the technique used to stop the flow, the stopped flow does result in increased sensitivities compared to normal FIA.

The traditional stopped flow FIA systems also have the advantage of being able to assay samples sequentially at speeds up to 2 samples per minute with a relatively simple apparatus. However, the reagent-sample peak profiles of stopped flow FIA have not been demonstrated to exhibit the conditions of physical steady state.

-Different FIA Manifold Designs

Many research papers on FIA have been written describing sample dispersion and possible ways to counter its deleterious effects. For example, control of sample dispersion was attempted by varying the reaction coil length and the use of flow reversals.[31] Also investigated to improve FIA laminar dispersion was the design of different FIA manifold embodiments, mostly altering the reaction coil length.[32] Most recently however, data processing techniques for FIA have been investigated for mathematically predicting physical steady-state signal attainment for the improvement of linear ranges.[33,34]

The prelude paper to the development of the ByT-FAS flow system by Korenaga *et al* examined the reduction in tubing internal diameter, length, detector volumes and flow rates for their effects on peak shapes.[35] From the results of this paper, the genesis of the concept and successful design of ByT-FAS emerged. With the advent of the highest-sensitivity, absolute measurement non-segmented continuous flow analyzer, ByT-FAS, new theoretical limits to miniaturization, initially postulated by van der Linden, will need to be put forth.[36]

Table A.1 (see Appendix) is a comparison of ByT-FAS to the analytical instruments described above in the areas of absolute measurements, sample throughput, automation potential, and approximate sample volumes.

Enzymes in Wet Chemistry Assays

The use of enzymes as analytical tools for the quantitation of analytes (kinetic or end-point equilibrium), both organic and inorganic, has a broad literature base.[37] To successfully use an

enzymatic assay for metabolite quantitation, several questions must be addressed:[38]

1. Is the enzyme specific for the desired analyte?
2. Is the enzyme affinity for the analyte of interest (substrate) sufficiently high (small enough Km)?
3. Does the enzyme have enough activity?
4. Is the reaction equilibrium favorable?
5. Is reaction monitoring on an appropriate time scale?

-Kinetic Based Metabolite Quantitation

Kinetic based quantitation of sample analytes is a widely used method of analysis and has a broad base of interest among clinical chemistry laboratories.[39] One reason kinetic methods have been employed rather extensively in clinical laboratories is their relative speed for each measurement compared with end-point methods. They are also extensively used to make enzyme activity measurements in the diagnosis of illness.[40,41]

A recent review of kinetic methods of analysis cited approximately 56 individual compounds for which kinetic protocols exist for quantitation.[42] Many of the compounds have more than one method and a few have as many as a dozen.

Kinetic methods for the determination of analyte concentrations measure reaction rate. The two types of kinetic reactions that are most useful in the quantitation of metabolites are zero-order reactions and first or pseudo-first-order reactions.

-Zero-order Kinetic Reactions

The rate of a zero-order reaction, by definition, is independent of the concentration of the reactant. As a result, the concentration of a reactant cannot be measured directly from the reaction rate. However, there is a direct relationship between a zero-order reaction and the activity of a catalyst. Therefore, it is possible to kinetically determine the concentration of a substance indirectly if it has an activating or inactivating effect on a catalyst. For example, a method for the determination of organophosphorus and carbamate insecticides based on their inhibition of the enzyme choline esterase has been described.[43] Even though some methods do exist for kinetic determination of analytes using zero-order reactions, they have found limited acceptance for routine determinations.

-First-order and Pseudo-first-order Kinetic Reactions

According to the Michaelis-Menten equation,

$$v_0 = Vmax(S)/[Km + (S)] \qquad (1.2)$$

the initial velocity (v_0) of an enzyme catalyzed reaction is a function of the kinetic constants (Vmax and Km) of the enzyme under specific reaction conditions and the concentration of the substrate (S) (reactant). When the concentration of the substrate (S) is significantly smaller than the Km value [(S) < or = 0.2 Km], then the above equation approximates,

$$v_0 = Vmax(S)/Km \qquad (1.3)$$

which produces a linear relationship between enzyme v_0 and substrate concentration (first-order reaction rate) with a slope of Vmax/Km. When (S) >> than Km, the Michaelis-Menten equation becomes,

$$v_0 = Vmax \qquad (1.4)$$

obeying zero-order reaction kinetics. As a result, the initial case when (S) is less than or equal to 0.2 Km, can provide a range of concentrations over which a linear standard curve can be generated using enzyme initial velocity and substrate (S) concentration.

For one-enzyme one-substrate reaction mixtures, the assay is straightforward; such reactions are rare. However, for reactions involving either more than one enzyme (coupled enzyme assay) or more than one substrate (bi-substrate reaction), the reaction mixture must be manipulated to behave as if it were a first-order reaction (pseudo-first-order reaction).

The technique employed to generate a pseudo-first-order reaction in an enzyme assay is to supply all the necessary substrates and enzymes other than the studied analyte in saturating concentrations. This will make the reaction involving the desired substrate and enzyme the rate-limiting step in reaction. The initial velocity of the reaction will be limited by the availability of the substrate of interest and the enzyme that consumes it. Coupled enzyme assays and/or bi-substrate reactions must be manipulated to behave as pseudo-first-order reactions to obtain useful initial velocities for the generation of a kinetic standard curve.[44]

One method to make linear the typical hyperbolic Michaelis-Menten plot of enzyme initial velocities versus substrate concentration is to use a double-reciprocal (Lineweaver-Burk) plot. While this data manipulation technique is most useful in evaluating the kinetic parameters of an enzyme, it has significant drawbacks for use as a standard curve in the quantitation of metabolite concentrations.

All enzyme velocity measurements have error associated with them. Typically, the smaller the reaction rate, the larger the relative error of the velocity. Taking the reciprocal of small velocities with large relative errors makes the double-reciprocal regression line for a standard curve too imprecise for metabolite quantitation.

-Fast-equilibrium End-point Based Metabolite Quantitation

A plethora of enzymatic end-point methodologies and/or diagnostic kits for the quantitation of numerous biochemical metabolites are available. However, most methods for these assays involve lengthy incubation times of 20 to 60 minutes for the attainment of reaction equilibrium. This is due to the economic consideration of the cost of the enzyme necessary to make the reaction attain equilibrium faster. However, most of the procedures are designed to use several hundred microliters to milliliters of sample for each assay.

If the sample size needed for utilization of these procedures were drastically reduced (10 to 100 times less), then the corresponding amount of enzyme consumed would also be reduced. The reduction in amount of enzyme needed could provide the opportunity for increasing the concentration of enzyme (in the smaller volume) to attain chemical equilibrium faster.

ByT-FAS has significantly smaller sample and reagent volume requirements than the traditional, manually performed methodologies. As a result, it is more feasible to increase the concentrations of enzymes in the assay to attain reaction equilibrium faster, without increasing the overall amount of enzyme used. This would not increase the cost of the assay.

In an enzyme catalyzed reaction where the starting substrate concentration is in the range of less than 0.2 times the Km value of the substrate for the enzyme, the laws for first-order reactions are approximately valid for calculating the time to attain the end-point of the reaction.[45] From this approach the ratio, Vmax/Km of the Michaelis-Menten equation becomes critical where Vmax is the catalytic concentration (units) of the enzyme used in the assay. When the substrate concentration is less than 0.2 times the Km value, then the ratio of Vmax/Km approximates the rate constant of an uncatalyzed first-order reaction and would be described by the first-order rate law;[45]

$$-d(S)/dt = k(S)$$

integrated to

$$(S) = (S_0)e^{-kt}$$

and rearranged to

$$\ln (S) = \ln (S_0) - kt \qquad \text{or}$$
$$t = 1/k \ln(S_0)/(S)$$

when $(S_0) < 0.2$ Km then k = Vmax/Km approximately, so

$$t = (Km/Vmax) \ln(S_0)/(S) \qquad (1.5)$$

From equation 1.5, the time to reach chemical equilibrium is a function of the Km of the substrate, the catalytic concentration of enzyme present, and the natural log of the ratio of initial substrate concentration to final substrate concentration.

A chemical reaction, catalyzed or uncatalyzed, approaches the concentrations present at equilibrium asymptotically. As a result it is not practical to wait until complete equilibrium is reached to obtain a quantitative measurement. A reaction that is 99% complete, is in most cases acceptable for taking an end-point measurement. Therefore, with the criterion of 99% of the original substrate concentration converted to product for determining the time of reaction completion, equation 1.5 reduces to;

$$t = (Km/Vmax) \ln 100 \qquad (1.6)$$

If the criterion for taking the reaction end-point method were 99.9% completion, then the last part of the reaction would be ln 1000, or an increase in time needed of 50% to go from 99% to 99.9%.

Its arguable whether such a small difference of measurement would be discernible or worth the significant extra investment of time.

Materials and Methods

Materials

Supplies

ByT-FAS flow system components including fingertight fittings (10.32 coned, 1/16" OD), T intersections (0.5 mm i.d.), cross (0.5 mm i.d.), PEEK system tubing (0.0025", 0.005", and 0.01" i.d., 1/16" OD), and flangeless ferrules and fittings (for 1/16" OD), were purchased from Upchurch Scientific (Oak Harbor, WA). Electronically actuated three-way valves were purchased from NResearch (W. Caldwell, NJ). Six port injection valves model number 7010 were purchased from Rheodyne (Cotati, CA).

Two different pump systems were used with the flow system. The large volume ByT-FAS system used a double head, 10 *u*L stroke Sanuki Series DMX Model DMX2300-T HPLC pump (Tokyo, Japan). The small system employed an infusion/withdrawal syringe pump model 980761 purchased from Harvard Apparatus (South Natick, MA). Syringes used in the syringe pump were Hamilton 1000 Series gastight with metal plunger assemblies and were purchased from Fisher Scientific (Pittsburgh, PA).

The UV/VIS spectrophotometer was a Gilford 260 model 1281X3 (Oberlin, OH). The HPLC fluorometer was a McPherson model FL-748 (Acton, MA).

Spectrophotometric detection employed the use of a Helma flow cell with 1 mm i.d. and a 1 cm path length. The HPLC fluorescence detector quartz flow cell was 0.8 mm i.d. for the large system and a 0.45 mm i.d. flow cell was custom manufactured and purchased from Wilmad glass (Buena, NJ) for the small system.

Chemicals

Chemical reagents were purchased from Fisher Scientific and Sigma Chemical Company. Canine heparinized plasma samples were provided as a gift from the college of veterinary medicine teaching hospital, Virginia Tech. *E. coli* strains containing the luciferase plasmid were provided as a gift from the laboratory of Dr. Timothy J. Larson (Biochemistry, Virginia Tech). Additional reagents and equipment are reported throughout this study followed in parenthesis by the supplier.

Computer Hardware and Software

The ByT-FAS flow system's electrical components (three-way valves, detector output) were interfaced to an IBM compatible 386 computer via a Data Translation DT2805 board (Marlborough, MA). LabTech Notebook version 6.0 was purchased from Laboratory Technologies Corporation (Wilmington, MA), and was used for data acquisition and system control. The duration of each ByT-FAS time period was predetermined and the three-way valves were programmed to fire accordingly using a binary ASCII file. Each successive data set generated was collected from the detector during a ByT-FAS run and was written by LabTech Notebook to a sequentially numbered ASCII file for future analysis. The numbered ASCII data sets were imported into Quattro Pro version 5.0 (Borland, St. Louis, MO) for quantitative analysis and interpretation.

ByT-FAS Instrument Design

Due to research developments with the ByT-FAS instrument concept through experimentation, two different ByT-FAS designs were used during the course of these studies. From this point forward, the two different instrument embodiments will be referred to as the large ByT-FAS and small ByT-FAS system accordingly.

Critical Flow Area

The critical flow area of a ByT-FAS system is defined as those parts of the system that contribute to sample and reagent dispersion from the point of injection to detection. The critical flow area for both the large and small ByT-FAS embodiments is the same. However, some different component parts were used (i.e. tubing with smaller internal diameters) in the separate embodiments. Wherever possible in the critical flow area (sample and reagent coil loops, mixing coil) tubing was braided and knotted to disrupt laminar flow.

Large ByT-FAS Design

A schematic diagram of the large ByT-FAS flow instrument concept is shown in Figure 2.1. All component parts of the system (pumps, valves, tubing sections, sample injection valves, T's , Cross, and detector cell) are labeled.

The large ByT-FAS flow system used a double head 10 *u*L stroke HPLC pump. The flow rates for the reagent and sample carrier flow streams were approximately the same and were calibrated for experimental data analysis.

From Figure 2.1, the critical flow area for the large system is comprised of component part numbers 5, 6, 7, 9, 10, 15, 16, 17, 19, 20, and 21. The tubing component numbers 6, 9, 16, and 19 were 0.25 mm i.d. by 1/16" OD by 5 cm long. The T's and Cross, component numbers 7, 17, and 10 were 0.5 mm i.d. Tubing component number 20 was the mixing coil and was 0.305 mm i.d. by 18 cm long, and braided. The detector cell was a Helma spectrophotometric flow cell with 1 mm i.d. and a 1 cm path length. The inlet tubing to the Helma flow cell was 0.5 mm i.d. by 10 cm long and not braided. The fluorometric detector cell for the large system was quartz and 0.8 mm i.d. by 2 cm long.

For the large ByT-FAS system, as shown in Figure 2.1, the sample and reagent carrier flow streams meet at the cross in a head-on manner.

Small ByT-FAS Design

A schematic diagram of the small ByT-FAS flow instrument concept is shown in Figure 2.2. All component parts of the system (pumps, valves, tubing sections, sample injection valves, T's , Cross, and detector cell) are labeled.

The small ByT-FAS system employed an infusion/withdrawal syringe pump to deliver a continuous flow for the sample and reagent carrier flow streams. The reagent and sample carrier flow streams were pumped at different flow rates by using different volume syringes

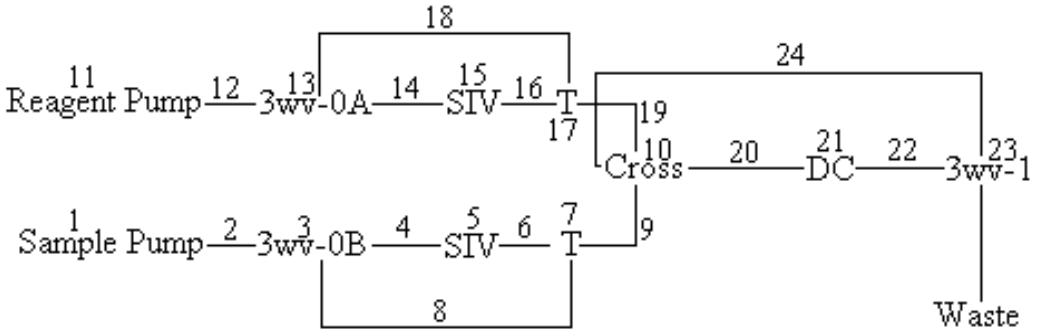

Figure 2.1. Schematic diagram of a Large ByT-FAS flow system.
All component parts and tubing sections labeled by number. Approximately equal flow rates are used for both the sample carrier flow stream and the reagent carrier stream. At the point of mixing in the cross the flow streams are merged in a head on manner. Critical flow area is comprised of component numbers 5, 6, 7, 9, 10, 15, 16, 17, 19, 20, and 21. 3wv-0A - three way valve for reagent injection valve, 3wv-0B - three way valve for sample injection valve, SIV- standard six port injection valve, T - three way intersection (0.5 mm i.d.), Cross - four way intersection (0.5 mm i.d.), DC - detector flow cell, 3wv-1 - three way valve controlling bypass flow.

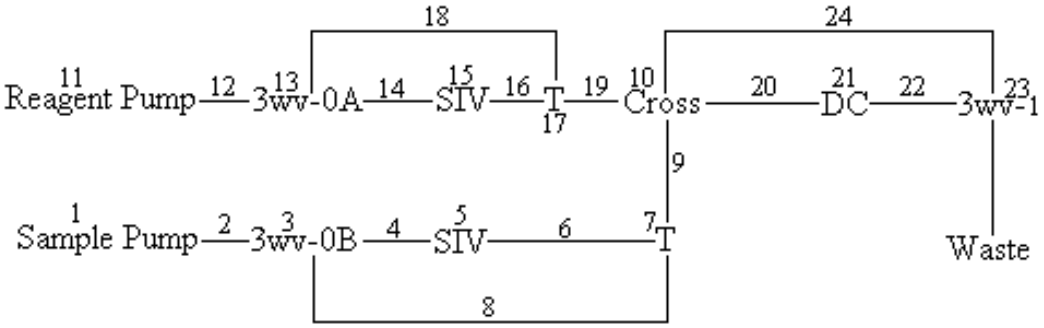

Figure 2.2. Schematic diagram of a Small ByT-FAS flow system.
All component parts and tubing sections are labeled by number. A ratio of flow rates are used for the sample and reagent carrier streams. At the point of mixing in the cross the flow streams are merged at a right angle to one another. Critical flow area is comprised of component numbers 5, 6, 7, 9, 10, 15, 16, 17, 19, 20, and 21. 3wv-0A - three way valve for reagent injection valve, 3wv-0B - three way valve for sample injection valve, SIV- standard six port injection valve, T - three way intersection (0.5 mm i.d.), Cross - four way intersection (0.5 mm i.d.), DC - detector flow cell, 3wv-1 - three way valve controlling bypass flow.

for the sample and reagent carrier reservoirs. The reagent and sample carrier flow streams were varied in a ratio from 10/1 to 2.5/1. Specifically, the reagent carrier flow stream had a flow rate of ten times that of the sample carrier flow stream. For example, the 10/1 ratio of reagent to sample carrier flow rate was achieved by using a 25 mL syringe for the reagent carrier reservoir and a 2.5 mL syringe for the sample carrier reservoir. During the course of experimentation, the syringe pump would displace 25 mL of solution through the reagent side of the system and 2.5 mL through the sample side.

From Figure 2.2, the critical flow area for the small ByT-FAS system is comprised of component part numbers 5, 6, 7, 9, 10, 15, 16, 17, 19, 20, and 21. The tubing component numbers 6, 9, 16, and 19 were 0.125 mm i.d. by 1/16" OD by 5 cm long. The T's and Cross, component numbers 7, 17, and 10 were 0.5 mm i.d. Tubing component number 20 was the mixing coil and was 0.125 mm i.d. by 12 cm long and braided**.** The detector cell was a quartz HPLC fluorometric flow cell of 0.45 mm i.d. by 2 cm long .

For the small ByT-FAS system, as shown in Figure 2.2, the sample and reagent carrier flow streams are merged in the cross at right angle to one another.

ByT-FAS Flow Control

The flow control of a ByT-FAS assay run is the same for both the large and small flow system embodiments.

The flow of the reagent and sample carrier streams through the system is controlled by firing the three-way valves 3, 13, and 23 in Figure 2.2. These three-way valves are programmed to divert flow using binary ASCII files read by LabTech notebook during a ByT-FAS run.

There are five stages of flow control during a ByT-FAS assay run. These are; Prerun/(Sample Loading/Reagent Loading), Sample/Reagent Loading or Injection (Parts 1 and 2), Attainment of Physical Steady State, Product (or Analyte) Detection, and System Flush. The control of flow through each part of the system is shown in Table 2.1. Schematic

Table 2.1: Flow Control of a ByT-FAS Assay Run.

Stage	SIVs-Sample Loop Position	Critical Flow Component in or out of Flow Stream	
		SIV(s)	Detector
PRERUN (Figure 2.3)			
(**Sample Loading/Reagent Loading)**			
Load Sample-Loop (Figure 2.3)	Load	In-stream	In-stream
Load Reagent -Loop (Figure 2.3)	Load		
SAMPLE/REAGENT LOADING OR INJECTION (Figures 2.4 and 2.5)			
Part 1			
Sample-Loop Loaded (Figure 2.4)	Load	Bypass	In-stream
Reagent-Loop Loaded (Figure 2.4)	Load		
Part 2			
Sample-Loop Injected (Figure 2.5)	Inject	Bypass	In-stream
Reagent -Loop Injected (Figure 2.5)	Inject		
ATTAINMENT OF PHYSICAL STEADY STATE (Figure 2.6)			
Sample-Loop Injected (Figure 2.6)	Inject	In-stream	In-stream
Reagent- Loop Injected (Figure 2.6)	Inject		
PRODUCT (or ANALYTE) DETECTION (Figure 2.7)			
	Inject	In-stream	Bypass
SYSTEM FLUSH - PRERUN (Figure 2.3)			
(Sample Loading/Reagent Loading)			
Load Sample-Loop (Figure 2.3)	Load	In-stream	In-stream
Load Reagent-Loop (Figure 2.3)	Load		

diagrams of the flow through each part of the system during the five stages are shown in Figures 2.3, 2.4, 2.5, 2.6, and 2.7.

The first stage of a ByT-FAS run is the Prerun (Sample Loading/Reagent Loading) shown in Figure 2.3 and described in Table 2.1. The sample and reagent loops in the standard injection valves (SIVs) are in the load position (Figure 2.3) and out of the flowing stream. The carrier flow streams are pumped through the sample and reagent SIVs but not the sample and reagent loops and through the detector cell (Figure 2.3). During this stage the sample and reagent are loaded into their respective loops in the SIVs.

After the sample and reagent loops are loaded, the ByT-FAS timing sequence is initiated to begin the Sample/Reagent Injection (Parts 1 and 2) stage. Two seconds after the timing sequence has begun, the system flow is switched from the Prerun flow pattern to bypass the sample and reagent injection valves by electronically switching the three-way valves upstream (3WV-0A and 3WV-0B) of the SIVs as shown in Figure 2.4 (See Table 2.1). This is Part 1 of the Sample/Reagent Injection stage of a ByT-FAS run. Once the flow has been directed around the SIVs, the SIVs sample and reagent loops are manually switched into the inject position as shown in Figure 2.5. This is Part 2 of the Sample/Reagent Injection stage of a ByT-FAS run. The Sample/Reagent Injection stage (Parts 1 and 2) occupies seconds two through six of a ByT-FAS run.

After the sample and reagent loops have been injected, the flow pattern of the system is changed to that shown in Figure 2.6 by electronically switching the SIVs three-way valves (3WV-0A and 3WV-0B). This marks the beginning of the Attainment of Physical Steady State stage of a ByT-FAS run (See Table 2.1). During this stage the sample and reagent boluses travel through the T's, meet at the cross, mix together, and travel into and through the detector flow cell (DC) as shown in Figure 2.6. If the injected sample and reagent volumes are large enough, and the ByT-FAS embodiment is sufficiently designed with the appropriate geometry, the concentration of a portion of the mixed bolus will reach a physical steady state profile in the detector cell.

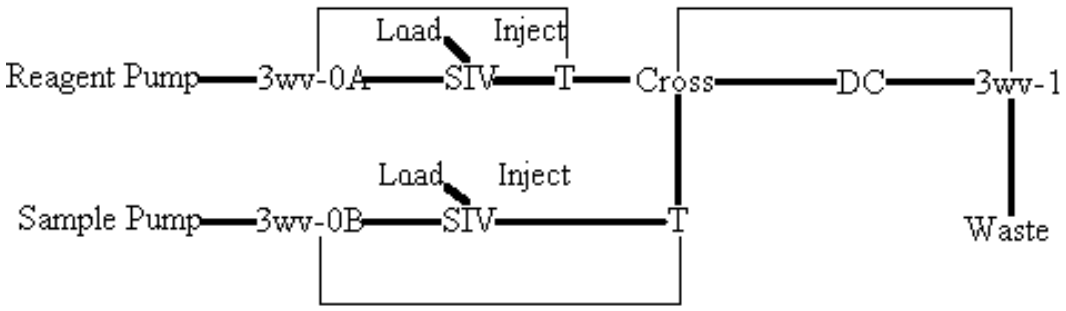

Figure 2.3. Prerun, Sample Loading/Reagent Loading,

--------- Not in flow stream. ▬▬▬▬▬ In flow stream.

3wv-0A - three way valve for reagent injection valve, 3wv-0B - three way valve for sample injection valve, SIV- standard six port injection valve, T - three way intersection (0.5 mm i.d.), Cross - four way intersection (0.5 mm i.d.), DC - detector flow cell, 3wv-1 - three way valve controlling bypass flow. See Table 2.1.

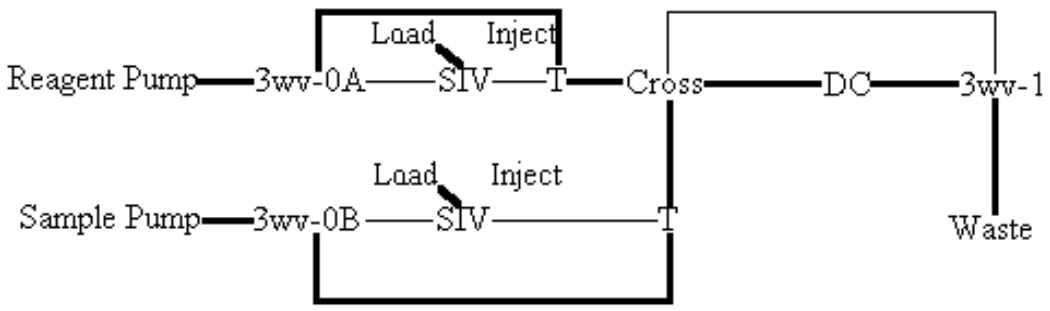

Figure 2.4. Sample/Reagent Loading or Injection , Part 1.

---------- Not in flow stream. ▬▬▬▬▬▬▬▬ In flow stream.

3wv-0A - three way valve for reagent injection valve, 3wv-0B - three way valve for sample injection valve, SIV- standard six port injection valve, T - three way intersection (0.5 mm i.d.), Cross - four way intersection (0.5 mm i.d.), DC - detector flow cell, 3wv-1 - three way valve controlling bypass flow. See Table 2.1.

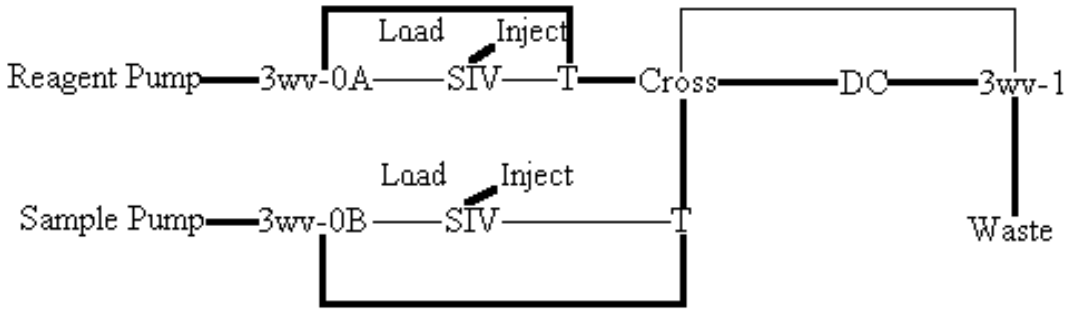

Figure 2.5. Sample/Reagent Loading or Injection, Part 2.

---------- Not in flow stream. ▬▬▬▬▬▬ In flow stream.

3wv-0A - three way valve for reagent injection valve, 3wv-0B - three way valve for sample injection valve, SIV- standard six port injection valve, T - three way intersection (0.5 mm i.d.), Cross - four way intersection (0.5 mm i.d.), DC - detector flow cell, 3wv-1 - three way valve controlling bypass flow. See Table 2.1.

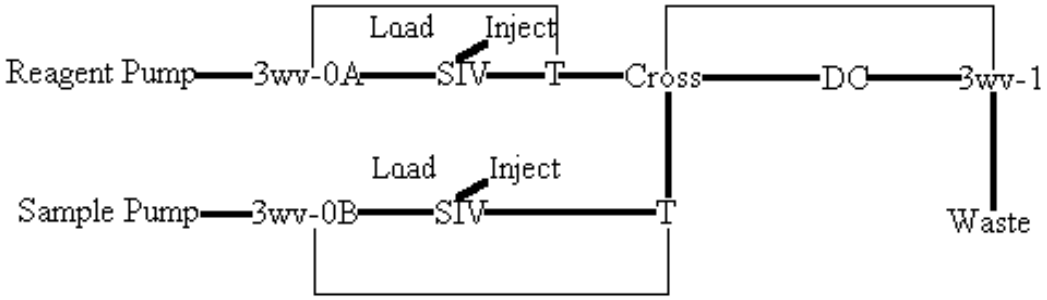

Figure 2.6. Attainment of Physical Steady State.

---------- Not in flow stream. ========== In flow stream.

3wv-0A - three way valve for reagent injection valve, 3wv-0B - three way valve for sample injection valve, SIV- standard six port injection valve, T - three way intersection (0.5 mm i.d.), Cross - four way intersection (0.5 mm i.d.), DC - detector flow cell, 3wv-1 - three way valve controlling bypass flow. See Table 2.1.

Once a physical steady-state concentration has been attained, the ByT-FAS run will begin the Analyte Detection stage (See Table 2.1). The flow pattern of the Analyte Detection stage is obtained (Figure 2.7) by firing the 3-way valve (3WV-1) downstream of the detector flow cell to **bypass** the detector cell and **trap** the physical steady state concentration in the detector cell. After sufficient data have been taken in the detector cell, the downstream 3WV-1 is switched back to end the Analyte Detection stage of the run.

This begins the System Flush stage of the ByT-FAS assay run. The System Flush stage has a flow pattern identical to that of the Prerun (Sample Loading/Reagent Loading) stage as shown in Figure 2.3. During System Flush stage, the detector cell is flushed of analytes to return the detector reading back to a baseline value, ready for another assay. Either during the System Flush stage or after the run has been completed, the sample and reagent SIVs may be switched from the Inject position to the Load position for a new assay.

The needed length of each stage is dependent upon any given ByT-FAS design and geometry, the sample carrier stream flow rate, the reagent carrier stream flow rate, the assay chemistry reaction rates, sample and reagent analyte molecular weights, and the amount of data needed for a given assay. Thus, different assay types, or different analytes may require distinct ByT-FAS stage time durations.

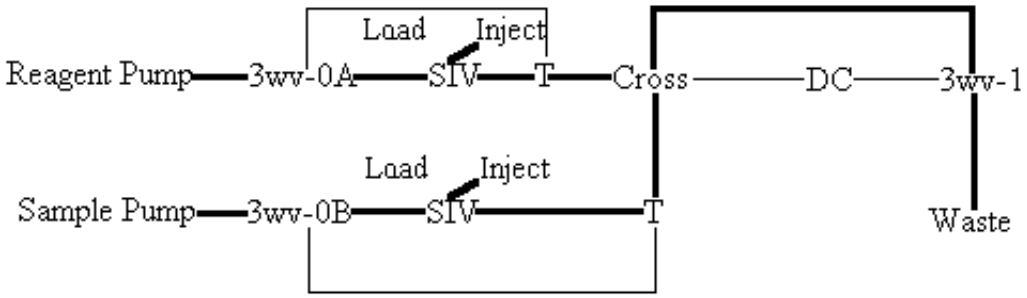

Figure 2.7. Analyte Detection.

---------- Not in flow stream. ▬▬▬▬▬▬ In flow stream.

3wv-0A - three way valve for reagent injection valve, 3wv-0B - three way valve for sample injection valve, SIV- standard six port injection valve, T - three way intersection (0.5 mm i.d.), Cross - four way intersection (0.5 mm i.d.), DC - detector flow cell, 3wv-1 - three way valve controlling bypass flow. See Table 2.1.

Methods

Preparation of Solutions

All solutions were prepared using distilled water. The pH was adjusted prior to bringing the solution to final volume. Storage conditions depended on the solution. Solutions were stored at room temperature (~15 - 25°C), in the refrigerator at 4°C, or in the freezer at -20°C. If needed, the solutions were protected from light by storage in dark bottles.

Methods for Large ByT-FAS Design

1.1 Direct Hemoglobin Measurements

Hemoglobin solutions of 0.015, 0.03, 0.06, 0.1, 0.15, and 0.2 mg/ml were prepared in duplicate in 0.05 M NaCl. Each solution's absorbance at 405 nm was measured by injection into the sample side of ByT-FAS and by direct manual measurement using cuvettes. The ByT-FAS sample and reagent carrier streams were both 0.05 M NaCl. The total flow rate of the system was 1 mL/min. Standard curves for hemoglobin concentration were generated from the ByT-FAS physical steady state absorbance and the manually measured data. The standard curves were compared for limits of detection (LOD), R^2, and linear range.

1.2 Brom-Cresol Green (BCG) Equilibrium Protein Assay

The manual method dilutes the protein sample with BCG reagent in a 1/2 ratio. Because the large ByT-FAS system mixes the sample with reagent in approximately a 1/1 ratio, a modified BCG reagent was prepared so that the ratio of sample to reagent at the point of detection would be the same for both methods. The manual method was then modified to use the same BCG reagent by changing the mixing ratio of sample to reagent to 1/1 also. This made a direct comparison of the two methods as unambiguous as possible.

Solutions of bovine serum albumin (BSA) at 0.05, 0.1, 0.2, 0.4, 0.8, 1, and 2.0 mg/ml were prepared in duplicate in 0.05 M NaCl. The BCG reagent was prepared as follows; 133 mg BCG, 2.66 gm NaOH, 13.07 gm succinate, 2.0 gm Brij 35, to 1 liter of distilled water, adjusted pH to 4.05. Each BSA sample was assayed by a 200 *u*L injection into the sample side of ByT-FAS and manually by adding an equivalent ratio of BCG reagent as occurred in-flow. BCG reagent was pumped from the reagent and sample carrier stream reservoirs into ByT-FAS to mix with the injected BSA samples. The total flow rate of the system was 1 mL/min. Standard curves for BSA concentration were generated from the ByT-FAS equilibrium data and the manually pipetted data. The standard curves were compared for LOD, R^2, and linear range.

1.3 Enzyme Velocity as a Function of Alkaline Phosphatase Concentration

A glycine buffer was prepared with the following components and concentrations, 50 mM glycine, 1 mM $MgSO_4$, 0.1 mM $ZnSO_4$ and adjusted to pH 10 with NaOH.
4 mM *p*-nitrophenylphosphate (*p*-NPP) was prepared in glycine buffer. Solutions of alkaline phosphatase (EC 3.1.3.1) at 0, 10.5, 21.1, 31.6, 42.2, and 52.7 *u*g/mL were prepared in duplicate from an alkaline phosphatase stock of 0.25 mg/mL. 200 *u*L of the 4 mM *p*-NPP solution was

injected in the sample side of ByT-FAS and 200 *u*L of the alkaline phosphatase solutions were injected into the reagent side of the system. The reagent and sample carrier stream solution was glycine buffer. The total flow rate of the system was 1 mL/min. Alkaline phosphatase velocity was measured by trapping the reaction in the detector flow cell between 32 and 52 seconds into the run.

1.4 Alkaline Phosphatase Velocity as a Function of *p*-NPP Concentration

The glycine buffer described above was used for this assay as well. Solutions of *p*-NPP at 0.5, 0.6, 0.75, 1, 1.33, and 2 mM were prepared in glycine buffer in duplicate from a 4 mM stock solution. A 20 *u*g/mL solution of alkaline phosphatase was prepared for use as the sample solution. 200 *u*L of the *p*-NPP samples was injected into the reagent side of ByT-FAS and 200 *u*L of the alkaline phosphatase solution was injected into the sample side of the system for each run. The reagent and sample carrier stream solution was glycine buffer. The total flow rate of the system was 1 mL/min. Alkaline phosphatase velocity was measured spectrophotometrically at 400 nm in the detector flow cell between 32 and 52 seconds into the run. For comparison of the ByT-FAS generated data to manually generated kinetic data, 1 mL of each *p*-NPP solution was added to 1 mL of 20 *u*g/mL alkaline phosphatase in a cuvette, mixed, and assayed for enzyme velocity in a spectrophotometer at 400 nm with a chart recorder.

1.5 Dilution Adjustment to Alkaline Phosphatase Velocity as a function of *p*-NPP Concentration and addition of 0.1% BSA to assay mixture.

All components of this assay are identical to the one above except as noted below. Since the ByT-FAS reagent to sample carrier stream flow ratio was 52.7% to 47.3% as shown by the direct hemoglobin concentration measurements, the manual assay was adjusted to have an enzyme to substrate ratio of 47.3% to 52.7% (0.946 mL alkaline phosphatase to 1.054 mL of *p*-NPP) to directly compare to the ByT-FAS generated data. Also, all component solutions of the assay were made in the presence of 0.1% BSA (1 mg/mL).

1.6 Fluorescence Detection Additivity of Fluorescence for Calibration of Flow Ratio

Using the McPherson Model FL-748 HPLC fluorometer with a 0.8 mm internal diameter flow cell, 200 *u*L of a quinine tracer of 4 ng/mL was injected into the sample side of the system alone, then the reagent side alone, and then both simultaneously to determine additivity of fluorescence. The reagent and sample carrier flow stream solution was 0.1N H_2SO_4. The total flow rate of the system was 1 mL/min.

1.7 Visible Inspection of Quinine to Physical Steady State

Using the McPherson Model FL-748 HPLC fluorometer with a 0.8 mm internal diameter flow cell, 200 *u*L of a quinine tracer of 4 ng/mL was injected into the sample side of the system to visibly inspect when the fluorescent signal reached physical steady state in the detector cell. The reagent and sample carrier flow stream solution was 0.1N H_2SO_4.
The total flow rate of the system was 1 mL/min.

1.8 Fluorometric Coupled Enzyme Assay of Hexokinase

All enzyme and substrate solutions were prepared and assayed in 50 mM MOPS (3- [N-morpholino]propanesulfonic acid) buffer and 1 mM $MgCl_2$ at pH 7.4. The source of hexokinase (E.C. 2.7.1.1.) and glucose-6-phosphate dehydrogenase (G6PDH) (E.C. 1.1.1.49) used in all assays was yeast. $NADP^+$, ATP, and ADP were also used as substrates or inhibitors in the assays of hexokinase with ByT-FAS instrumentation . All sample and reagent solutions were filtered at 0.8 *u*m before use with ByT-FAS.

The assay of hexokinase velocity as a function of hexokinase concentration was performed at concentrations of 0.5, 1.0, 2.0, 4.0 and 5.0 Units/mL injected. The concentrations of G6PDH and all substrates in the reaction were fixed at 5 Units/mL and 5 mM respectively. For this assay all reaction components except hexokinase were mixed together and 200 *u*L were injected as the reagent. 200 *u*L of hexokinase was injected alone as the sample. The reagent and sample carrier stream solution was the MOPS buffer. The velocity of hexokinase was monitored fluorometrically in the detector cell by the accumulation of reduced NADPH with an excitation wavelength of 340 nm and an emission wavelength of 460 nm.

1.9 Hexokinase Velocity as a Function of Glucose Concentration

The velocity of hexokinase as a function of glucose was measured with glucose concentrations of 0.020, 0.025, 0.033, 0.05, 0.066, 0.250, 1, and 2.5 mM injected. Hexokinase and G6PDH were fixed at 1 and 3.5 Units/mL injected respectively. The injected concentrations of $NADP^+$ and ATP were both 7.5 mM. The reagent for this assay was the mixture of both enzymes and $NADP^+$ and ATP while the sample (glucose) was injected alone. The reaction was monitored fluorometrically by the coupling enzyme product NADPH.

1.10 Hexokinase Velocity as a Function of ATP Concentration in the Presence of Competitive Inhibitor ADP

The velocity of hexokinase as a function of ATP concentration in the presence of the competitive inhibitor ADP was performed using ATP concentrations of 0.3, 0.6, 1.0, and 1.5 mM injected and ADP concentrations of 0, 1, 2, and 3 mM injected. The reagent for this experiment consisted of both enzymes and the substrates $NADP^+$ and glucose. The concentrations of the reagent analytes were 1 and 3.5 Units/mL of hexokinase and G6PDH respectively with 5 mM $NADP^+$ and glucose. Each ATP concentration was prepared in the presence of the different amounts of ADP described above. Each ATP/ADP mixture was then injected as the sample. The reaction was monitored fluorometrically by the coupling enzyme product NADPH.

Methods for Small ByT-FAS Design

2.1 Additivity of Fluorescence Investigation Using a Syringe Pump and Smaller Internal Diameter Tubing

Using a syringe pump with a 25 mL reagent carrier stream reservoir syringe and a 10 mL sample carrier stream reservoir syringe an additivity of fluorescence experiment was performed for the syringe pump's effects on the attainment of physical steady state. The injected tracer was 0.2

ng/mL quinine. The reagent and sample injection coil loops were reduced to 100 *u*L. The critical flow area tubing as described above and shown in Figure 2.1 was changed to 0.005" i.d. on both the sample and reagent sides of the system. The fluorescence detector flow cell was changed from 0.8 mm internal diameter to 0.45 mm. The reagent to sample carrier stream flow ratio was 2.5/1. The reagent and sample carrier flow streams met in the cross in a head-on manner as shown in Figure 2.1. First, quinine was injected into the sample side of the system alone, then the reagent side alone, and then both simultaneously to determine additivity of fluorescence. The reagent and sample carrier flow stream solution was 0.1N H_2SO_4. The total flow rate of the system was 1 ml/min.

2.2 Additivity of Fluorescence, Effects of Angle of Convergence at the Cross

The effects of changing the angle of convergence from head on as shown in Figure 2.1 to a 90° angle as shown in Figure 2.2 were investigated using exactly the same experimental conditions described in experiment 2.1.

2.3 Investigation of a 5 *u*L Fluorescent Tracer to Reach Physical Steady State

Using a 25 mL reagent carrier stream reservoir and a 2.5 mL sample carrier stream reservoir (reagent to sample carrier stream flow ratio of 10/1) multiple injections of a 5 *u*L quinine tracer into the sample side of the system were made at two different pump speeds. The two different total flow rates were approximately 0.22 mL/min and 0.11 mL/min. The reagent and sample carrier flow stream solution was 0.1N H_2SO_4.

2.4 Additivity of Fluorescence for 5 *u*L Sample Volume and 70 *u*L Reagent Volume

Using a syringe pump with a 25 mL reagent carrier stream reservoir syringe and a 2.5 mL sample carrier stream reservoir syringe an additivity of fluorescence experiment was performed to calibrate the reagent to sample carrier stream flow ratio. The injected tracer was 5 ng/mL quinine. The reagent coil loop was 70 *u*L and the sample coil loop was 5 *u*L. The critical flow area tubing as described above and shown in Figure 2.2 was 0.005" i.d. on the reagent side of the system and 0.0025" i.d. on the sample side of the system. The reagent to sample carrier stream flow ratio was 10/1. The reagent and sample carrier flow streams met in the cross at a 90° angle as shown in Figure 2.2. First, quinine was injected into the sample side of the system alone, then the reagent side alone, and then both simultaneously to determine additivity of fluorescence. The reagent and sample carrier flow stream solution was 0.1N H_2SO_4. The total flow rate of the system was 0.22 mL/min.

2.5 Sample Physical Steady State Validation With Absolute Measurement

Using 25 mL and 2.5 mL reagent and sample carrier stream reservoir syringes respectively, an absolute measurement of quinine in the system was made to calibrate the attainment of physical steady state with a 25 *u*L sample injection. Initially, a fluorometer baseline was established with both the reagent and sample syringes filled with 0.1N H_2SO_4 and pumped through the system for approximately 30 minutes. The reagent and sample coil loops were left continuously in the inject position. The 2.5 mL sample reservoir syringe was filled with 10 ng/mL quinine and inserted back into the syringe pump. The system flow was then initiated so that the quinine tracer would saturate

the sample side of the flow system and attain a steady absolute measurement in the detector cell. The system was run for approximately 30 minutes to stabilize and reach saturation of the quinine tracer in the detector cell. After 30 minutes, a data collection run of the fluorescence signal was initiated to measure the absolute quinine concentration in the detector cell.

The 2.5 mL syringe was then emptied of the quinine tracer and refilled with the 0.1N H_2SO_4 carrier solution. This was allowed to flow through the system for approximately 30 minutes to allow the detector to return to baseline and flush all of the quinine tracer out of the system. Once the detector had returned to baseline, 25 *u*L of the quinine solution used to fill the sample syringe reagent reservoir was injected into the system to determine when and if the sample reached physical steady state compared to the absolute measurement. Four 25 *u*L injections of the quinine sample were made. The reagent to sample carrier stream flow ratio was 10/1. The total system flow rate was 0.22 mL/min.

2.6 Low Molecular Weight Analyte; Effects of Sample Volume on Reaching Physical Steady State With 0.0025" Sample Side Tubing Internal Diameter

Using a reagent to sample carrier stream flow ratio of 10/1 (25 mL and 2.5 mL reagent and sample carrier stream reservoir syringes, respectively) the effects of injected sample volume on the attainment of physical steady state with a low molecular weight analyte was assayed. The sample side of the critical flow area used 0.0025" internal diameter tubing. Triplicate injections of 10 ng/mL quinine were made for sample coil loop volumes of 5, 10, 15, and 25 *u*L. The reagent and sample carrier flow stream solution was 0.1N H_2SO_4. The total system flow rate was 0.22 mL/min.

2.7 Low Molecular Weight Analyte; Effects of Sample Volume on Reaching Physical Steady State With 0.005" Sample Side Tubing Internal Diameter

Using a reagent to sample carrier stream flow ratio of 10/1 (25 mL and 2.5 mL reagent and sample carrier stream reservoir syringes, respectively) the effects of injected sample volume on the attainment of physical steady state with a low molecular weight analyte was assayed. The sample side of the critical flow area used 0.005" internal diameter tubing in place of 0.0025". Triplicate injections of 10 ng/mL quinine were made for sample coil loop volumes of 10, 15, and 25 *u*L. The reagent and sample carrier flow stream solution was 0.1 N H_2SO_4. The total system flow rate was 0.22 mL/min.

2.8 Low Molecular Weight Analyte; Effects of Sample Volume on Reaching Physical Steady State With Reagent to Sample Flow Stream Ratio of 5/1.

Using a reagent to sample carrier stream flow ratio of 5/1 (25 mL and 5 mL reagent and sample carrier stream reservoir syringes, respectively) the effects of injected sample volume on the attainment of physical steady state with a low molecular weight analyte was assayed. The sample side of the critical flow area used 0.005" internal diameter tubing. Triplicate injections of 10 ng/mL quinine were made for sample coil loop volumes of 10, 15, and 25 *u*L. The reagent and sample carrier flow stream solution was 0.1N H_2SO_4. The total system flow rate was 0.24 mL/min.

2.9 Low Molecular Weight Analyte; Effects of Sample Volume on Reaching Physical Steady State With Reagent to Sample Flow Stream Ratio of 2.5/1.

Using a reagent to sample carrier stream flow ratio of 2.5/1 (25 mL and 10 mL reagent and sample carrier stream reservoir syringes, respectively) the effects of injected sample volume on the attainment of physical steady state with a low molecular weight analyte was assayed. The sample side of the critical flow area used 0.005" internal diameter tubing. Triplicate injections of 10 ng/mL quinine were made for sample coil loop volumes of 15, 25, and 50 *u*L. The reagent and sample carrier flow stream solution was 0.1 N H_2SO_4. The total system flow rate was 0.28 mL/min.

2.10 High Molecular Weight Analyte; Effects of Reagent Volume on Reaching Physical Steady State With Reagent to Sample Flow Stream Ratio of 10/1.

Using a reagent to sample carrier stream flow ratio of 10/1 (25 mL and 2.5 mL reagent and sample carrier stream reservoir syringes, respectively) the effects of injected reagent volume on the attainment of physical steady state with a high molecular weight analyte was assayed. The reagent side of the critical flow area used 0.005" internal diameter tubing. Triplicate injections of fluorescein isothiocyanate bovine serum albumin (FITC-BSA) at 3 mg/mL were made for reagent coil loop volumes of 100 and 125 *u*L. FITC-BSA was dissolved in 50 mM Hepes buffer at pH 7.4 with 50 mM NaCl. The reagent and sample carrier flow stream solution was the 50 mM Hepes buffer. The total system flow rate was 0.22 mL/min.

2.11 Calibration of the Age of an Enzyme Reaction at the Time of Trapping at Physical Steady State

Using a reagent to sample carrier stream flow ratio of 10/1 (25 mL and 2.5 mL reagent and sample carrier stream reservoir syringes, respectively) the age of an enzyme catalyzed reaction at the point of trapping in the flow system was assayed. 100 *u*L of 0.1 U/mL yeast glucose-6-phosphate dehydrogenase (G6PDH) was injected into the reagent side of the system and 10 *u*L of a 10 mM glucose-6-phosphate and 10 mM $NADP^+$ solution was injected into the sample side of the system. The sample and reagent solutions were prepared in 50 mM Tris buffer at pH 8.0. The reagent and sample carrier flow stream solution was the 50 mM Tris buffer. Both sample and reagent blank runs were taken before a kinetic velocity was taken. The reagent and sample mixture bolus was trapped in the detector at 39 seconds. The total system flow rate was 0.22 mL/min. The enzyme reaction age was calculated as the difference between the reagent and sample mixture physical steady state signal (RSpss) and the enzyme control (E_c) signal divided by the initial velocity (V_0) reaction rate during trapping. This is equivalent to a linear back extrapolation to zero fluorescence which should be zero time for the enzyme reaction assuming no lag phase.

$$(RSpss - E_c) / V_0 \qquad (2.1)$$

2.12 Coupled Enzyme Kinetic Glucose Assay Standard Curve Development

Using the coupled enzyme reaction of yeast hexokinase and yeast G6PDH, a kinetic based standard curve was developed for the quantification of glucose as a metabolite in solution. The

velocity of hexokinase as a function of glucose concentration was measured with glucose at 0, 5, 10, 25, 40, and 50 *u*M at the point of detection. Because the reagent to sample carrier stream flow ratio was 10/1 (sample dilution of 1/11 at the point of detection), the injected glucose concentrations required to have the desired concentrations at the detector were 0, 55, 110, 275, 440, and 550 *u*M. Each glucose sample solution was assayed in duplicate. The reagent was composed of 0.25 U/mL hexokinase, 1.5 U/mL G6PDH, 2.5 mM $NADP^+$, and 2.5 mM ATP at the point of detection. Because the reagent to sample carrier stream flow ratio was 10/1 (reagent dilution of 10/11 at the point of detection), the injected reagent concentrations required to have the desired concentrations at the detector were 0.275 U/mL hexokinase, 1.65 U/mL G6PDH, 2.75 mM $NADP^+$, and 2.75 mM ATP. All enzyme and substrate solutions were prepared and assayed in 50 mM MOPS buffer and 1 mM $MgCl_2$ at pH 7.4. The reagent for this assay was the mixture of both enzymes and $NADP^+$ and ATP while the sample (glucose) was injected alone. 125 *u*L and 15 *u*L of reagent and sample were injected respectively for each assay run. The total system flow rate was 0.22 mL/min. The reagent and sample carrier stream solution was the MOPS buffer.

2.13 Manual Colorimetric Equilibrium Enzyme Assay of Starch Standards

Potato starch standard solutions of 0, 90, 170, 270, and 350 mg/mL were prepared in 50 mM sodium acetate buffer, pH 5.0, and digested to glucose with amyloglucosidase (EC 3.2.1.3) at 37°C overnight. The standard solutions were then assayed for glucose content with a coupled enzyme equilibrium assay. The reagent solution for the assay of glucose was composed of glucose oxidase (EC 1.1.3.4), horse radish peroxidase (EC 1.11.1.7), and the chromophore o-dianisidine. This reagent mixture was purchased pre-made from Sigma (St. Louis, MO) in the form of a diagnostic kit. 0.5 mL of the standard starch solutions was added to 2.5 mL of the reagent and incubated for 45 minutes at room temperature in the dark for color development to occur. The reaction was then quenched with 5 mL of 4N hydrochloric acid. The absorbance of each sample was then taken at 533 nm and put in the form of a standard curve.

2.14 Method of Standard Additions for the Coupled Enzyme Kinetic Assay of Glucose in Heparinized Canine Plasma

Heparinized canine plasma samples were obtained from the Virginia-Maryland Regional College of Veterinary Medicine. Two sets of glucose standard solutions were prepared. One set was to be the standard response glucose solutions and the other the standard additions set. The standard response glucose concentrations were prepared in duplicate and to achieve 0, 5, 10, and 25 *u*M at the point of detection. The standard additions set of glucose solutions were prepared in duplicate and to achieve 0, 5, 7.5, and 10 *u*M at the point of detection. To each solution of the standard additions, enough heparinized plasma was added to increase the concentration of glucose at the detector by about 15 *u*M. As a result, the standard addition solutions would give a signals representative of 15, 20, 22.5, and 25 *u*M glucose at the point of detection. Both sets of solutions were then assayed with reagent and system settings as described above for the couple enzyme kinetic assay of glucose. Both sets of data from the coupled enzyme kinetic method were presented together to observe the effects the mixed diet food matrix may have had on the assay chemistry.

2.15 Fast Equilibrium Coupled Enzyme Assay of Cholesterol; Standard Curve Development

Using a coupled enzyme assay of cholesterol oxidase (EC 1.1.3.6) and horseradish peroxidase (EC 1.11.1.7) a fast equilibrium based standard curve was developed for the quantitation of cholesterol in a non-aqueous solution. The equilibrium fluorescence signal as a function of injected cholesterol concentration was quantification. The buffer solution was composed of 0.1 M potassium phosphate buffer at pH 7.4 with 10 mM sodium cholate to act as a detergent. The enzyme concentrations at the point of injection were 1.2 U/mL of cholesterol oxidase and 24 U/mL of peroxidase. The fluorophore of the reaction mixture was *p*-hydroxyphenylacetic acid (*p*-HPA) and was injected with the reagent at a concentration of 3 mM. Cholesterol stock solution was prepared in 95% ethanol at 1 mM. Cholesterol was assayed at concentrations of 0, 1.1, 4.1, and 8.2 *u*M at the point of detection. The reagent to sample carrier stream flow ratio was 10/1 (25 mL and 2.5 mL reagent and sample carrier stream reservoir syringes respectively). The reagent carrier stream solution was the assay buffer system while the sample carrier stream solution was 95% ethanol. 125 *u*L and 15 *u*L of reagent and sample were injected respectively for each assay run. The total system flow rate was approximately 0.22 mL/min.

2.16 Chemiluminescent Assay of ATP with Firefly Luciferase

ATP solutions of 0, 25, 75, 150, 300, 500, and 750 nM were prepared and assayed by injection into the reagent side of the system. The ATP solutions were prepared in a buffer solution of 40 mM Tris, 2 mM EDTA, 5 mM $MgSO_4$, and 0.1% BSA. The reagent, composed of a firefly (*Photinus pyralis*) luciferase (EC 1.13.12.7) and luciferin powder mix, was purchased from Sigma (Catalog #L-9314), dissolved in water, and injected into the sample side of the system at 8 mg/mL. A reagent to sample carrier stream flow ratio of 10/1 (25 mL and 2.5 mL reagent and sample carrier stream reservoir syringes respectively) was used. The ATP solutions were injected into the reagent side of the system using a 100 *u*L reagent loop coil, and the enzyme /coenzyme reagent was injected into the sample side of the system using a 10 *u*L sample loop coil. The detector used to measure light production from the reaction was the HPLC fluorometer described previously, without the light source turned on. Also, the face plate blocking the excitation light from the photomultiplier tube under normal operation was removed to allow direct exposure of the flow cell to the light detector. The reagent and sample carrier flow stream was the Tris buffer described above. The total flow rate of the system was 0.22 mL/min.

2.17 Whole *E. coli* cell Chemiluminescent Assay of Genetic Transcription Levels

E. coli strain pUHE2 P_{N25}/tetO_4Luci was obtained as a gift from the laboratory of Dr. Timothy J. Larson. This strain of *E. coli* contains a plasmid with kanamycin resistance and a gene for firefly luciferase under the transcription control of tetracycline. The strain has approximately 80 to 100 copies of the plasmid per cell. The bacterial strain was sustained on LB Agar (20 gm/L LB Lennox broth, 15 gm/L Agar) plates with 50 *u*g/mL kanamycin by reinoculation every 2 -3 weeks. The strain was assayed for the level of luciferase transcription as a function of tetracycline induction. The *E.coli* level of genetic transcription of luciferase was assayed was follows. LB broth was

prepared containing 50 ug/mL kanamycin and 0, 50, 75, and 100 ng/mL tetracycline. One colony of *E. coli* was picked from the agar plate using a P-200 pipette tip and dropped in the LB broth for each tube. The cultures were incubated for growth overnight at 37°C under continuous shaking. After overnight incubation (16 hours), the tubes were removed from 37°C and set at room temperature (20°C) for approximately 2 hours.

The cooled cultures were then diluted 1/25 into fresh LB broth and measured for their absorbance at 600 nm versus an LB broth blank. The diluted whole cell *E. coli* cultures were then assayed in the flow system for light production. The cells were injected into the reagent side of the system with a reagent coil loop of 125 *u*L. Luciferin at 1 mM dissolved in water was injected into the sample side of the system using a sample coil loop of 15 *u*L. The reagent and sample carrier stream solution was LB broth. The reagent and sample carrier stream flow ratio was 10/1. The total flow rate of the system was 0.22 mL/min. The detector used to measure chemiluminescent light production from the cells was the same as for the ATP assay.

Physical steady state signals for the injected whole cell cultures was not verified in these experiments. However, the ByT-FAS system still had adequate sensitivity for the analysis of luciferase in the whole cells.

Results

Large ByT-FAS Design

1.1 Direct Hemoglobin Measurements

The manual and ByT-FAS generated standard curves for hemoglobin absorbance at 405 nm as a function of concentration are shown in Figure 3.1. The data for the assay of the concentrations of hemoglobin at 405 nm calculated from the standard curves are shown in Table 3.1. As is shown, the manual and ByT-FAS methodologies yielded virtually identical results for LOD, R^2, and linear range in these assays. The difference in sensitivities is a result of the approximate 1/1 mixing of injected samples in ByT-FAS with the reagent carrier stream.

Table 3.1 Direct hemoglobin measurements comparison of manual and ByT-FAS data.

	Hemoglobin Assay	
	Manual	ByT-FAS
LOD (mg/mL)	0.0056	0.0039
R^2	0.999335	0.999674
Linear Range (mg/mL)	0.0056 - 0.2	0.0039 - 0.2
Sensitivity (AU/(mg/mL))	6.42	3.04

The different sensitivities (slopes) for the ByT-FAS and manual standard curves resulted from the dilution of the hemoglobin sample bolus with the reagent carrier flow stream at the cross. The dilution factor was approximately 1/2 for the large ByT-FAS system using the HPLC pump. However, for a flow system making absolute measurements, an approximation of the dilution factor occurring in ByT-FAS is not adequate. Therefore, this experiment can be used to calibrate the actual contribution of sample and reagent streams to the total flow rate. The ByT-FAS standard curve slope, expressed as a percentage of the

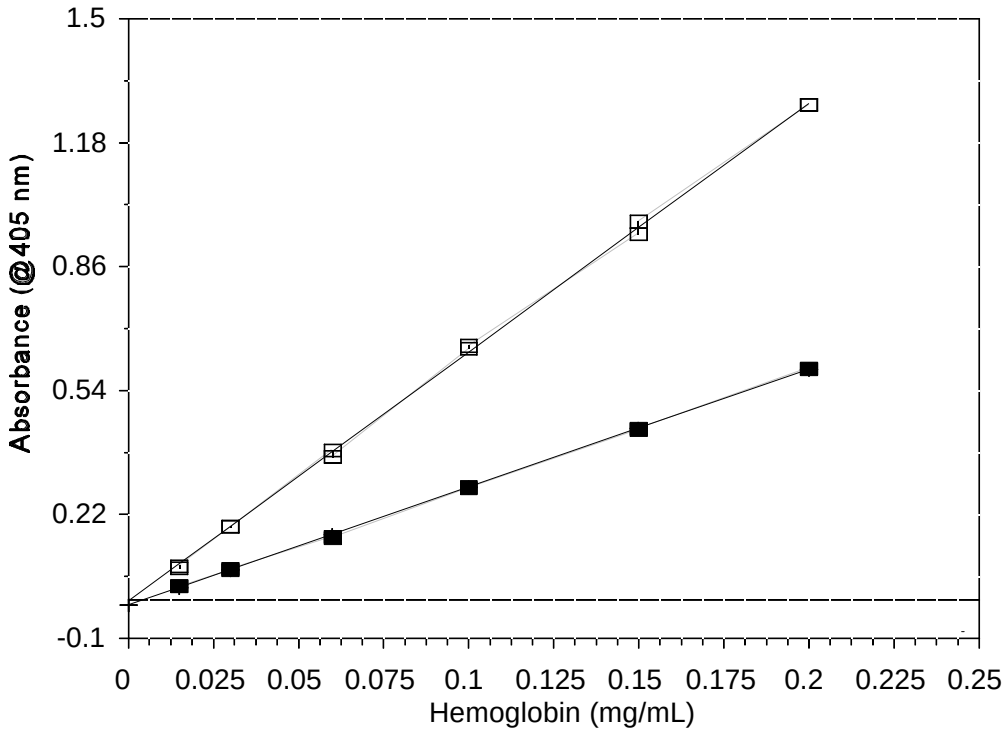

Figure 3.1 Comparison of ByT-FAS and manual direct hemoglobin measurements.

Large ByT-FAS system comparison of manual versus ByT-FAS spectrophotometric measurements. □ - Manual data, sensitivity = 6.42 AU/(mg/mL), LOD 0.0056 mg/mL. ■- ByT-FAS data, sensitivity = 3.04 AU/(mg/mL), LOD 0.0039 mg/mL. — Regression lines.

manual standard curve slope, can be used to determine the sample carrier stream flow rate as a percentage of the total flow rate if the measurements are indeed made at physical steady state. From Figure 3.1 the slope of the ByT-FAS standard curve is 3.04 AU/(mg/mL) and the manual slope is 6.42 AU/(mg/mL). This makes the ByT-FAS standard curve slope 47.3% of the manual standard curve slope. This indicates that the sample carrier flow stream contributes 47.3% of the total system flow rate while the reagent carrier flow stream contributes 52.7%.

1.2 Brom-Cresol Green Equilibrium Protein Assay

The manual and ByT-FAS generated standard curves for the Bromcresol green protein assay of BSA are shown in Figure 3.2. The data for the assay of the concentrations of BSA calculated from the standard curves are shown in Table 3.2. The manual and ByT-FAS methodologies yielded virtually identical results in these assays.

Table 3.2 Comparison of manual and ByT-FAS data for the BCG assay of BSA.

	BCG Assay of BSA	
	Manual	ByT-FAS
LOD (mg/mL)	0.015	0.012
R^2	0.999047	0.999373
Linear Range (mg/mL)	0.015 - 1	0.012 - 1
Sensitivity (AU/(mg/mL))	1.11	1.06

For the purpose of directly comparing the manual and ByT-FAS generated absorbances the BCG reagent was mixed with the BSA samples in a combination of 52.7% to 47.3% respectively to the total assay volume. This was done because the ByT-FAS system has a reagent contribution of 52.7% to the total system flow rate as determined from experiment

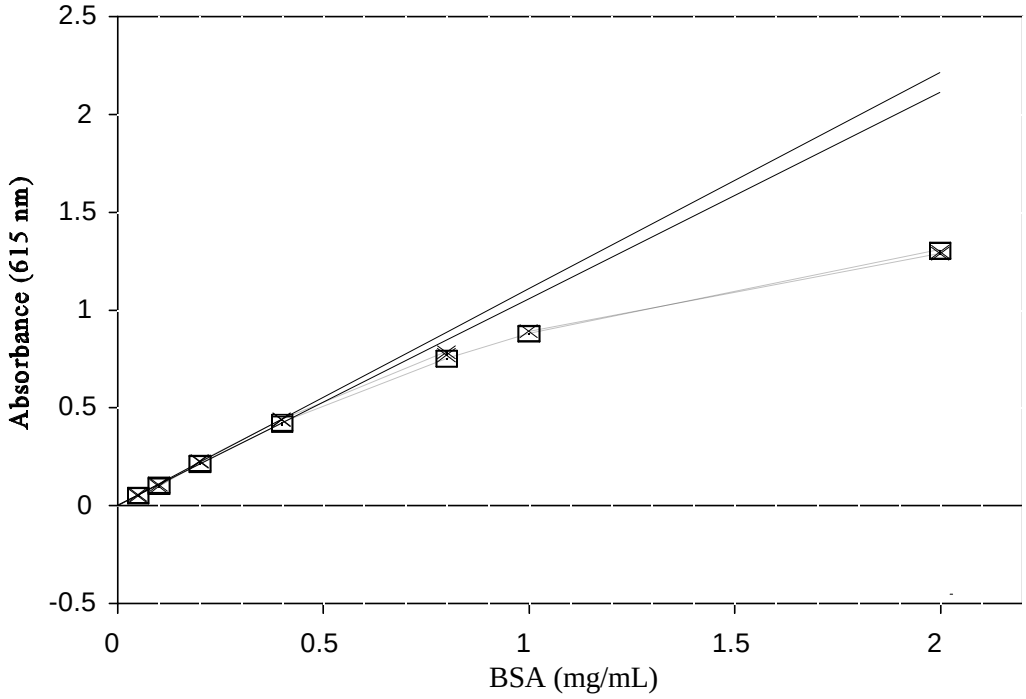

Figure 3.2. ByT-FAS versus manual Bromcresol Green (BCG) protein assay.

Large ByT-FAS system comparison of Bromcresol Green assay of bovine serum albumin, normalized manual assay data compared to ByT-FAS assay of same samples. □ - ByT-FAS data, sensitivity = 1.06 AU/(mg/mL), LOD 0.012 mg/mL. × - Manual data, sensitivity = 1.11 AU/(mg/mL), LOD 0.015 mg/mL. — Regression lines.

3.1. Using this method to facilitate direct comparison of the manual and ByT-FAS data, (Figure 3.2 and Table 3.2) the data obtained were virtually identical. This experiment validated the ability of the ByT-FAS flow system to match the sensitivity and precision of manual assay methodologies.

1.3 Enzyme Velocity as a Function of Alkaline Phosphatase Concentration

ByT-FAS data from the alkaline phosphatase velocity as a function of alkaline phosphatase concentration is shown in Figure 3.3. As expected the velocity of the catalyzed reaction was directly proportional to the concentration of enzyme. After achieving physical steady state, the enzyme velocity for each run was computed by regression analysis of the data during the trapped phase of the run. The unit of that regression analysis is absorbance /second, which corresponds to the rate of product production from the enzyme. The enzyme velocities were then plotted versus enzyme concentration. The concentrations of enzyme plotted on the X-axis of Figure 3.3 were the concentrations at the point of detection. The regression analysis of that graph gave a linear correlation coefficient of 0.986. From Figure 3.3, an enzyme concentration that gives a reasonable rate of production was chosen for the experiment of enzyme velocity as a function of *p*-NPP concentration.

1.4 Alkaline Phosphatase Velocity as a function of *p*-NPP Concentration

The Michaelis-Menten plot of alkaline phosphatase velocity as a function of *p*-NPP concentration generated from ByT-FAS and manual measurements is shown in Figure 3.4. The Lineweaver-Burk plot of the same data is shown in Figure 3.5. The ByT-FAS generated data reflects *p*-NPP concentrations that are assumed to be diluted 1/2 when they have reached the detector cell. However, as shown in experiment 1.1 above the reagent to sample carrier stream flow ratio for the large system was 52.7% to 47.3%. This partially explains why the ByT-FAS data is noticeably less than the manual data, which were generated with a reagent to sample ratio of 1/2. Because the *p*-NPP was injected in the reagent side of the system and

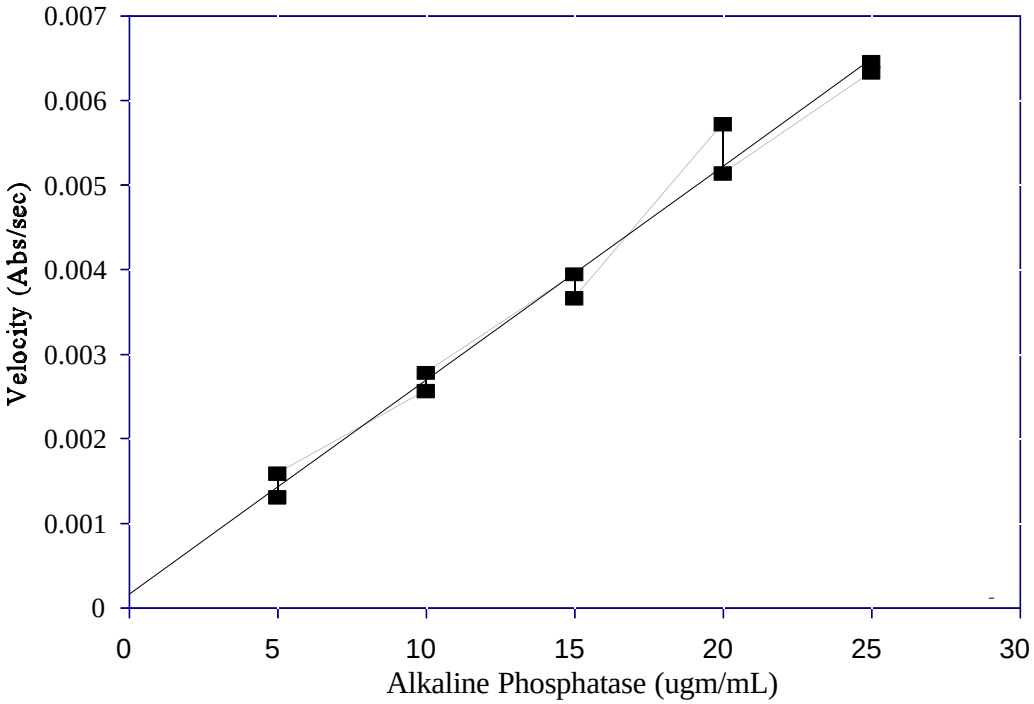

Figure 3.3. ByT-FAS alkaline phosphatase velocity as a function of enzyme concentration.

Large ByT-FAS system measurement of alkaline phosphatase velocity as a function of alkaline phosphatase concentration. Velocity of enzyme measured spectrophotometrically by the accumulation of phenolate anion at 400 nm. — Regression line.

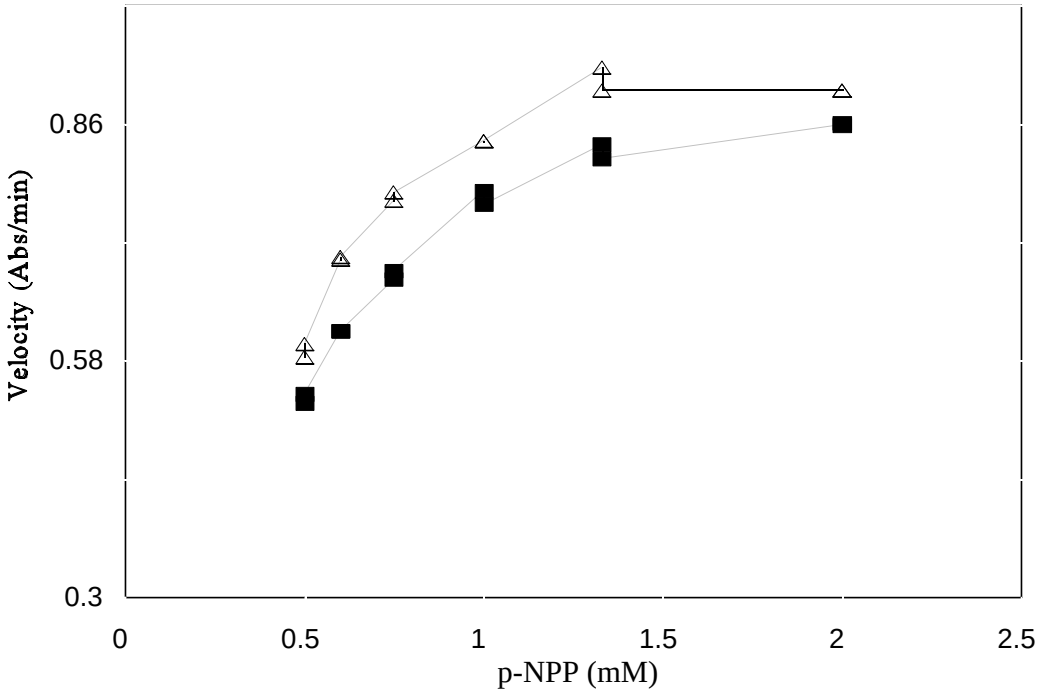

Figure 3.4. Michaelis-Menten plots of alkaline phosphatase velocity as a function of *p*-NPP performed manually and with large ByT-FAS system.

Comparison of ByT-FAS versus manually generated data. ■- ByT-FAS generated data.Δ- Manual data. Manual assay not adjusted for ByT-FAS reagent to sample carrier stream flow ratios.

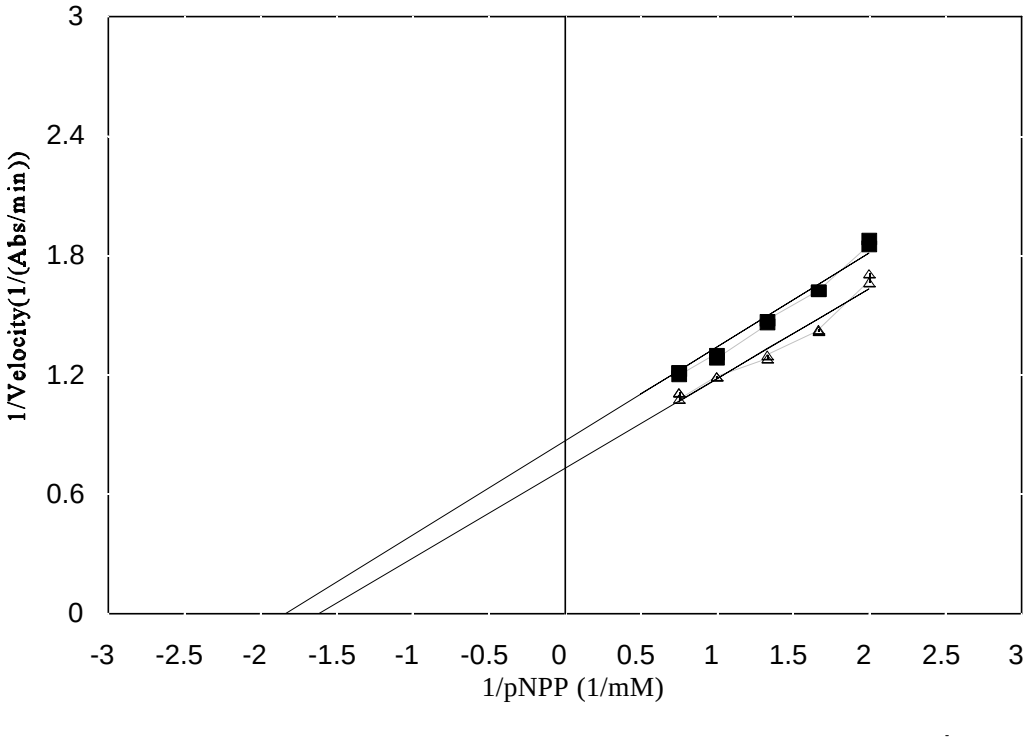

Figure 3.5. Lineweaver-Burk plot of alkaline phosphatase velocity as a function of *p*-NPP.

Comparison of ByT-FAS versus manually generated data. ■- ByT-FAS data.Δ- Manual data. Manual assay not adjusted for ByT-FAS reagent to sample flow ratios. — Regression lines.

the reagent contribution to the total system flow is 52.7%, the actual *p*-NPP concentrations at the detector cell in ByT-FAS are higher than were shown in Figures 3.4 and 3.5.

Also, the concentration of alkaline phosphatase at the detector cell was less than it was in the manual experiments because it was being injected into the sample side of ByT-FAS which was shown in experiment 1.1 to be 47.3% of the total system flow rate. As a result, the alkaline phosphatase concentration was not directly comparable with the manual measurement data. However, because the ratio of reagent to sample carrier flow streams is known, the ByT-FAS data can be adjusted for concentration measurements in an effort to make it comparable to the manual data. Shown in Figures 3.6 and 3.7 are the Michaelis-Menten and Lineweaver-Burk plots adjusted for the flow rate ratios in the ByT-FAS system. The concentrations of *p*-NPP at the detector cell are slightly more than shown in Figure 3.4 as a result of the higher reagent flow rate as a percentage of the total system flow rate. Also, the alkaline phosphatase velocities were adjusted and expressed as a velocity per amount of enzyme present at the point of detection. The velocity unit was changed from absorbance/minute in Figure 3.4 to (absorbance/minute)/(*u*g enzyme/mL) in Figure 3.6. These adjustments brought the ByT-FAS data closer to the manually generated data but did not close the gap entirely. The ByT-FAS alkaline phosphatase velocity still remained slower than the manual data.

1.5 Dilution Adjustment to Alkaline Phosphatase Velocity as a function of *p*-NPP Concentration and addition of 0.1% BSA to assay mixture

Because of the slower ByT-FAS enzyme velocities compared to the manual method, it was postulated that the alkaline phosphatase enzyme was undergoing nonspecific protein binding with the stainless steel tubing of the large ByT-FAS system. This would result in a decreased concentration of enzyme in the detector cell and therefore an attenuated velocity. To determine if nonspecific protein binding was occurring, the enzyme assay was performed in the presence of 0.1% BSA to saturate and block all potential protein binding sites in the ByT-FAS system. The manual assay was also performed in the presence of 0.1% BSA to ensure direct comparison to the ByT-FAS assay. The Lineweaver-Burk plot of the ByT-FAS

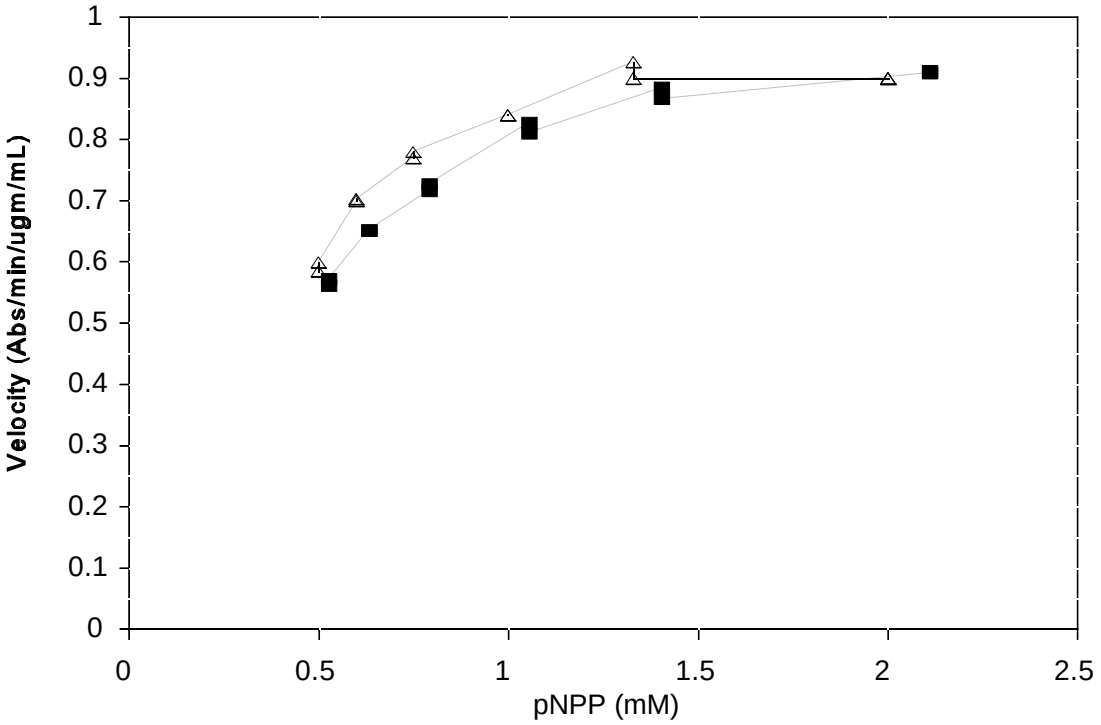

Figure 3.6. Michaelis-Menten plot of alkaline phosphatase velocity as a function of p-NPP.

Comparison of ByT-FAS versus manually generated data. ■- ByT-FAS generated data. Δ- Manual data. Manually performed assay adjusted for ByT-FAS reagent to sample carrier stream flow ratios.

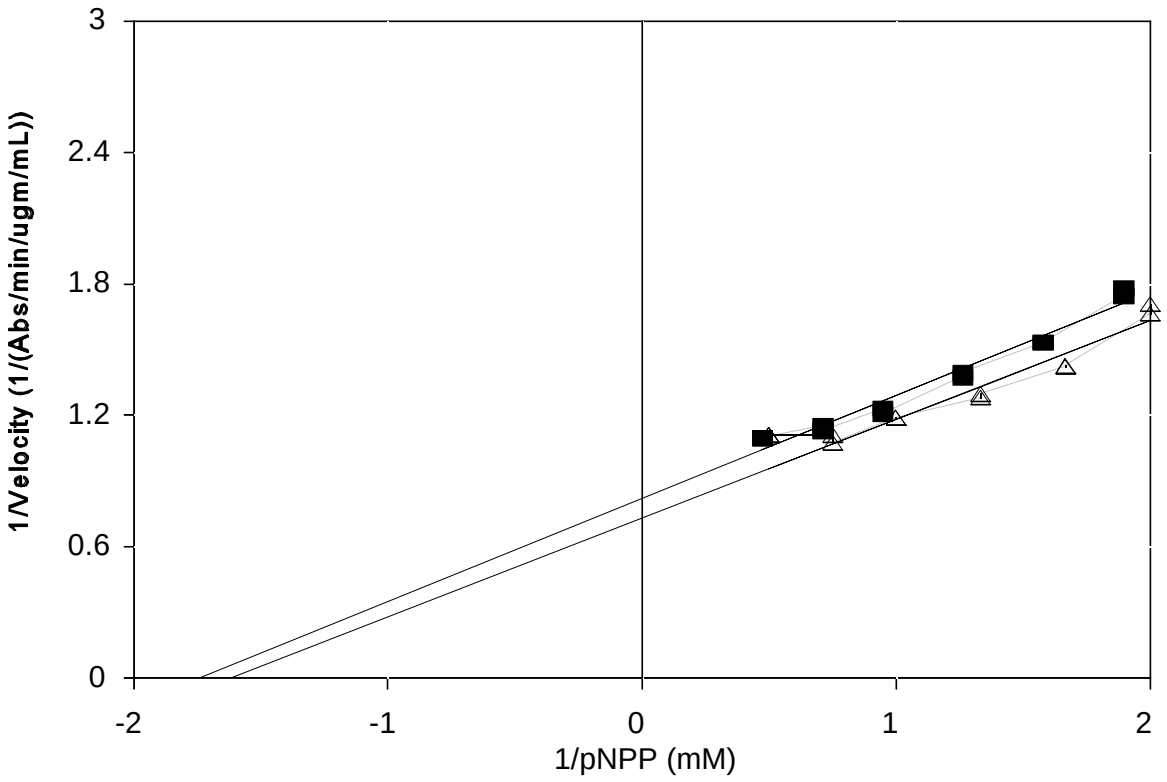

Figure 3.7. Lineweaver-Burk plot of alkaline phosphatase velocity as a function of *p*-NPP.

Comparison of ByT-FAS versus manually generated data. ■- ByT-FAS generated data. Δ- Manual data. Manually performed assay adjusted for ByT-FAS reagent to sample carrier stream flow ratios. — Regression lines.

and manual alkaline phosphatase data performed in 0.1% BSA is shown in Figure 3.8. The experiment was repeated for the demonstration of reproducibility and the Lineweaver-Burk plot shown in Figure 3.9 was generated. The raw data traces of the alkaline phosphatase assay performed on ByT-FAS are shown in Figure 3.10. The phenolate ion product of the reaction was measured by its strong absorbance at 400 nm at pH 10.

In addition to performing the assay in the presence of 0.1% BSA, adjustments were made to compensate for the ByT-FAS reagent and sample carrier flow stream ratios. The manual assay was performed by adding *p*-NPP to the enzyme in a final percentage of 52.7% to 47.3% of the assay's total volume respectively. This unequivocally made the ByT-FAS and manual data directly comparable.

The kinetic constants Vmax and Km for alkaline phosphatase by ByT-FAS and manual assay from replicate determinations on two separate days are shown in Table 3.3.

Table 3.3 Comparison of ByT-FAS versus manual techniques for the kinetic constants of alkaline phosphatase with *p*-NPP

	DAY 1		DAY 2	
	Km (mM)	Vmax (umol/min/mg)	Km (mM)	Vmax (umol/min/mg)
Manual	0.27 ± 0.051	17 ± 1.0	0.26 ± 0.060	16.0 ± 0.38
ByT-FAS	0.26 ± 0.005	17 ± 0.09	0.28 ± 0.020	16.6 ± 0.26

As is shown in Table 3.3, the ByT-FAS and manual techniques yield virtually identical results for the determination of alkaline phosphatase kinetic parameters. This validates the ability of ByT-FAS to make absolute measurements. However, as described above, appropriate care must be taken to ensure that the ByT-FAS measurements are directly comparable to manual techniques before using it exclusively in place of manual methodologies.

From Table 3.3, the ByT-FAS data has significantly smaller standard deviations than the

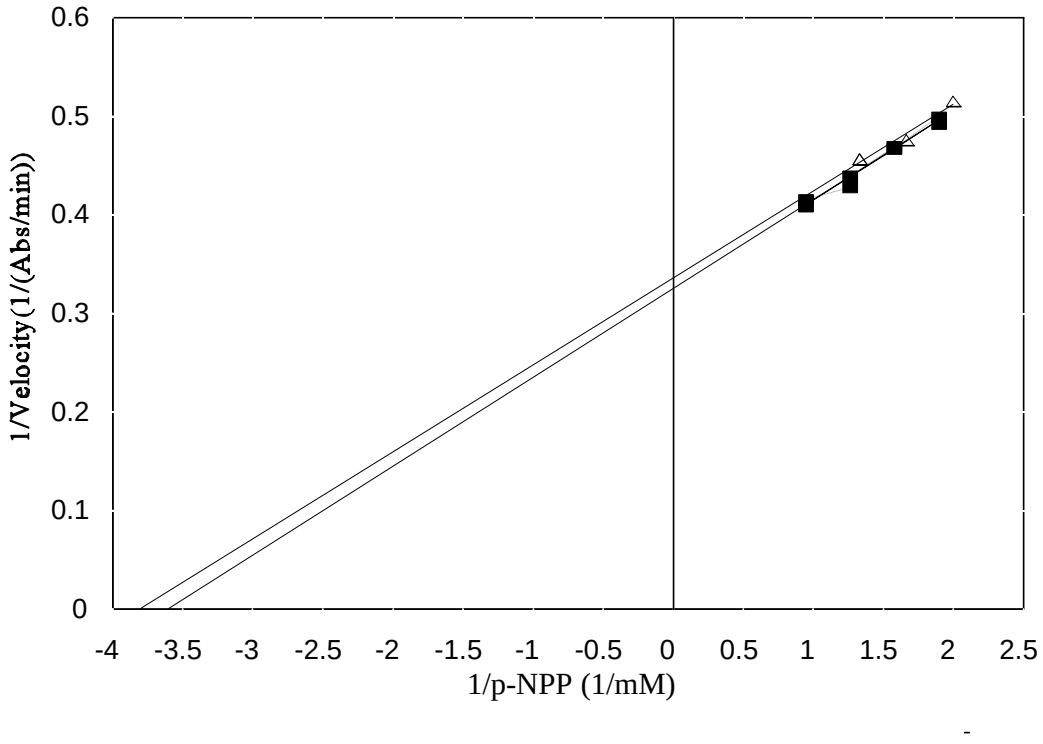

Figure 3.8. Lineweaver-Burk plot of alkaline phosphatase velocity as a function of *p*-NPP.

Comparison of ByT-FAS versus manually generated data. ■- ByT-FAS data. Δ- Manual data. Manual assay adjusted for ByT-FAS reagent to sample flow ratios. Bovine serum albumin was added to reaction solutions to block protein binding sites on stainless steel tubing in ByT-FAS system. — Regression lines.

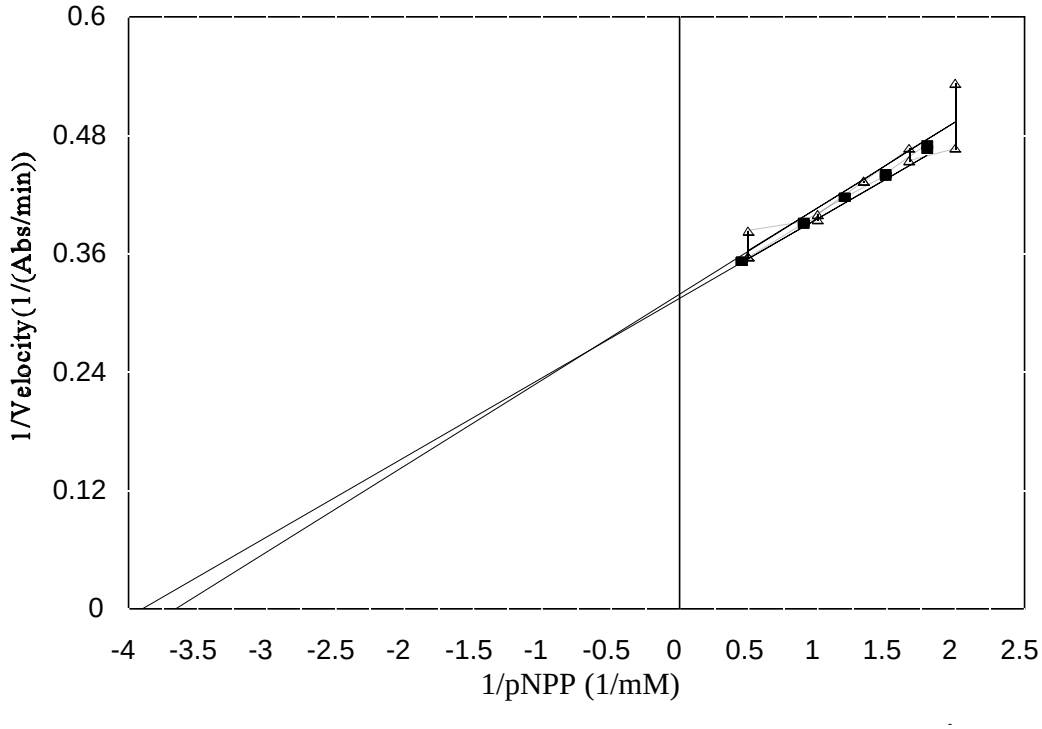

Figure 3.9. Lineweaver-Burk plot of alkaline phosphatase velocity as a function of *p*-NPP.

Comparison of ByT-FAS versus manually generated data. ■- ByT-FAS data. Δ- Manual data. Manual assay adjusted for ByT-FAS reagent to sample flow ratios. Bovine serum albumin was added to reaction solutions to block protein binding sites on stainless steel tubing in ByT-FAS system. — Regression lines.

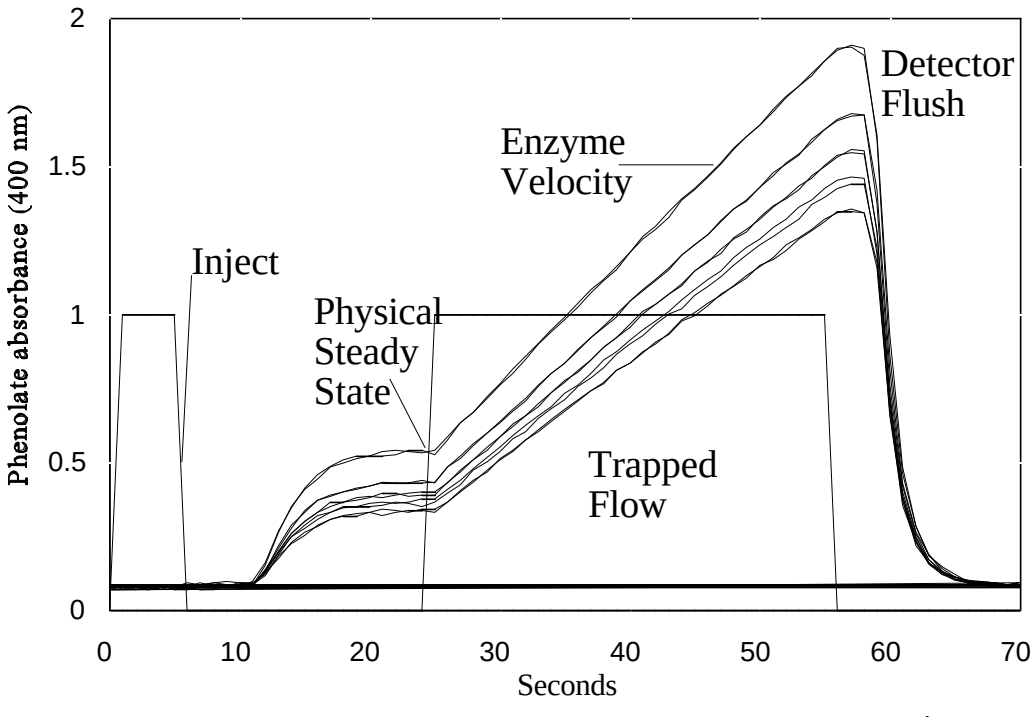

Figure 3.10. Alkaline phosphatase raw data velocities as a function of p-NPP concentration.

Large system ByT-FAS raw data for alkaline phosphatase velocities as a function of *p*-NPP concentration, with multiple assays plotted on the same graph. Duplicate assays for each *p*-NPP concentration. Increasing trapped flow slope corresponds to an increase in *p*-NPP concentration. Duplicate runs of each *p*-NPP concentration demonstrates good ByT-FAS measurement precision.

manual data for the calculated kinetic constants. This demonstrates that the ByT-FAS measurement precision is consistently equivalent to or better than manual assay precision.

1.6 Fluorescence Detection Additivity of Fluorescence for Calibration of Flow Ratio

Using the McPherson Model FL-748 HPLC fluorometer with a 0.8 mm internal diameter by 2 cm long flow cell, an additivity of quinine emission fluorescence was performed to calibrate the ratio of reagent to sample carrier flow stream contribution to the total system flow rate.

The raw data traces of the additivity of quinine fluorescence generated from ByT-FAS runs are shown in Figure 3.11. Because the configuration of the flow system was changed (different detector cell) it was necessary to investigate any changes in the contribution of reagent and sample carrier flow streams to the total flow rate. From Figure 3.11, it can be seen that the same quinine tracer injected separately (not simultaneously) into the reagent and sample sides of the system gave different fluorescent intensities in the detector cell. This indicated that the reagent and sample carrier flow stream contributions were not 50% each. However, the individual traces added together do match the signal from quinine injected into both sides simultaneously. Therefore, it is possible to calculate the percent of each reagent and sample injection to the total signal of a simultaneous injection. This will give the reagent and sample carrier flow stream percent contributions to the total flow rate. From Figure 3.11, the reagent quinine trace represented 52.8% of the simultaneous injection signal while the sample trace represented 47.2%. The reagent and sample carrier flow stream contributions for the fluorometric detector cell compare well to the reagent and sample carrier flow stream contributions with the spectrophotometric detector cell (experiment 1.1).

1.7 Visible Inspection of Quinine to Physical Steady State

A raw data plot of a quinine tracer is shown in Figure 3.12 to visually determine when physical steady state was obtained for a low molecular weight analyte. From this graph, the signal intensity with respect to the time of run does not change between approximately 25 and

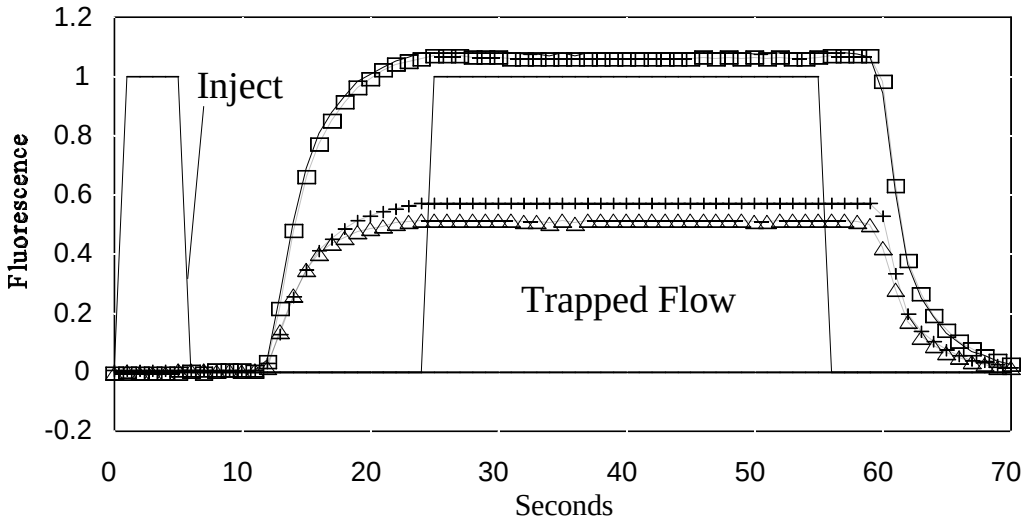

Figure 3.11. Fluorescence detection additivity of sample and reagent injection valves with large ByT-FAS system.

Large ByT-FAS system injections of quinine fluorophore into the reagent and sample carrier flow streams for calibration of flow rates with a fluorescent detector flow cell (0.8 mm i.d.). + - quinine injected with reagent injection valve only, Δ - quinine injected with sample injection valve only, □ - quinine injected into reagent and sample injection valve simultaneously, — Sum of reagent (+) ***and*** sample (Δ) raw data traces added together.

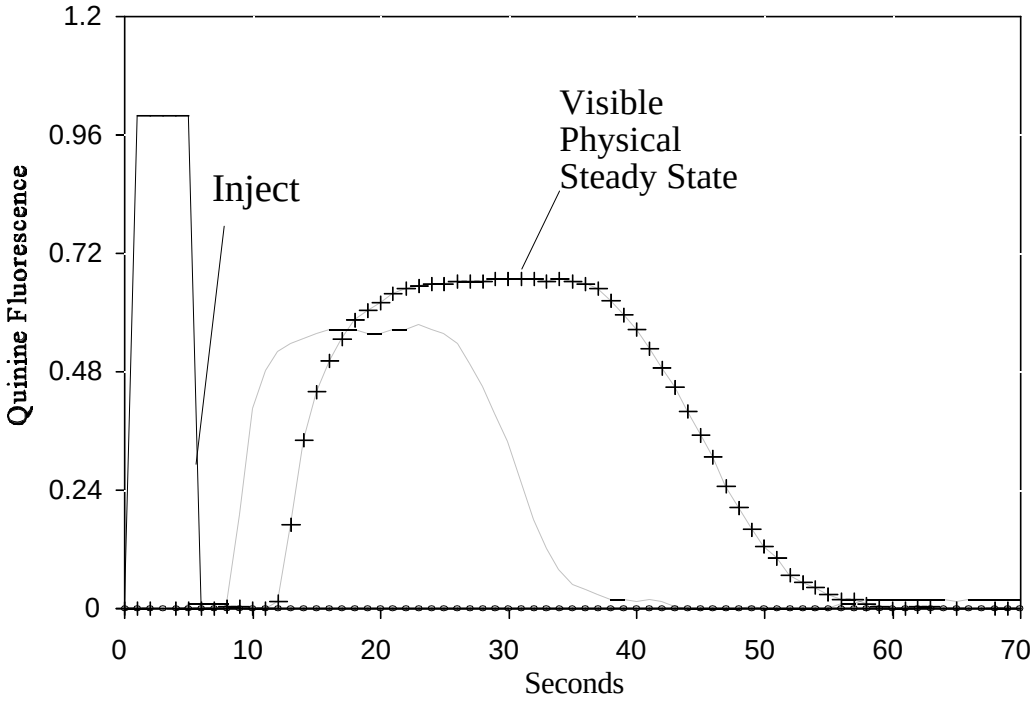

Figure 3.12. Large ByT-FAS system injection of a quinine tracer with fluorescence detection.

Large ByT-FAS system qualitative visible inspection of physical steady state attainment for injection of a 200 *u*L low molecular weight quinine tracer into the sample side of the system. Total flow rate of 1 mL/min. Qualitative determination of physical steady state between 25 and 35 seconds of the ByT-FAS run.

35 seconds. Therefore, the sample bolus is presumably at a physical steady state concentration in the detector cell for about 10 seconds of the ByT-FAS run. As will be shown below, a visible inspection of when physical steady state occurs for an injected bolus is not adequate.

1.8 Fluorometric Coupled Enzyme Assay of Hexokinase

To investigate the kinetic parameters of a given enzyme, the velocity of that enzyme must be the rate limiting step (pseudo-first-order) in the presence of other coupling enzyme(s). This experiment was performed to determine the concentration ratio of hexokinase to coupling enzyme that makes the hexokinase catalysis step the rate limiting step in the reaction. Shown in Figure 3.13 is a plot of hexokinase velocity as a function of hexokinase concentration in the reaction. From Figure 3.13 the hexokinase velocity is linear with respect to its own concentration up to 2 Units/mL. With the concentration of G6PDH fixed at 5 Units/mL, the ratio of hexokinase to coupling enzyme necessary to keep hexokinase the rate limiting step is 1/2.5. Concentrations of hexokinase above the 1/2.5 ratio would not make hexokinase the rate limiting step of the coupled enzyme reaction. In other words, if the relative concentration of hexokinase was higher than 1/2.5 the concentration of G6PDH, the velocity of hexokinase would not be a pseudo-first-order rate.

1.9 Hexokinase Velocity as a Function of Glucose Concentration

The Michaelis-Menten plot of hexokinase velocity as a function of glucose concentration is shown in Figure 3.14. The Lineweaver-Burk plot of the same data is shown in Figure 3.15. Figure 3.14 shows excellent saturation kinetics of hexokinase with glucose. The Km for glucose with yeast hexokinase was calculated from the Lineweaver-Burk plot to be 154 *u*M. This compares well with published values of the Km of hexokinase with glucose ranging from 100 *u*M to 170 *u*M.[46,47]

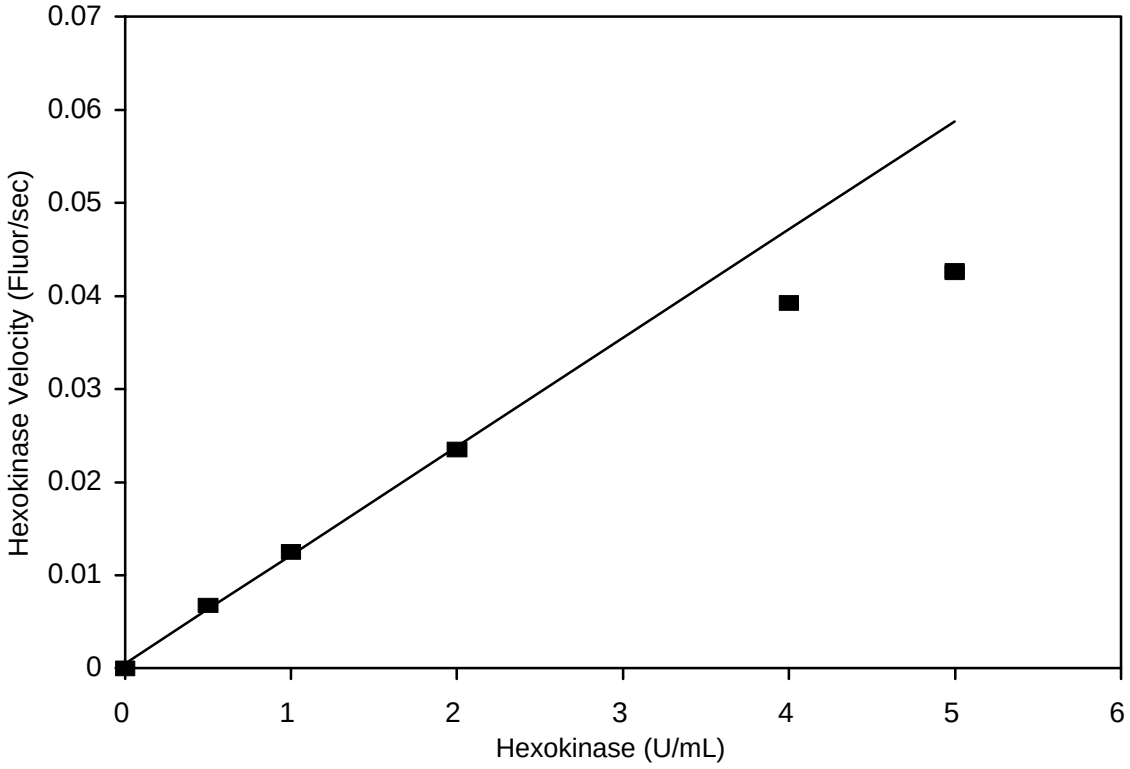

Figure 3.13. Large ByT-FAS system assay of hexokinase velocity as a function of hexokinase concentration.

Large ByT-FAS system elucidation of the ratio of hexokinase to coupling enzyme (glucose-6-phosphate dehydrogenase) to achieve a pseudo-first order reaction rate with respect to hexokinase. Glucose-6-phosphate dehydrogenase concentration held constant at 5 Units/mL. From the linear range high of 2 Units/mL hexokinase to 5 Units/mL G6PDH, to isolate the hexokinase velocity the hexokinase to coupling enzyme concentration ratio must be at most 1/2.5. — Regression line.

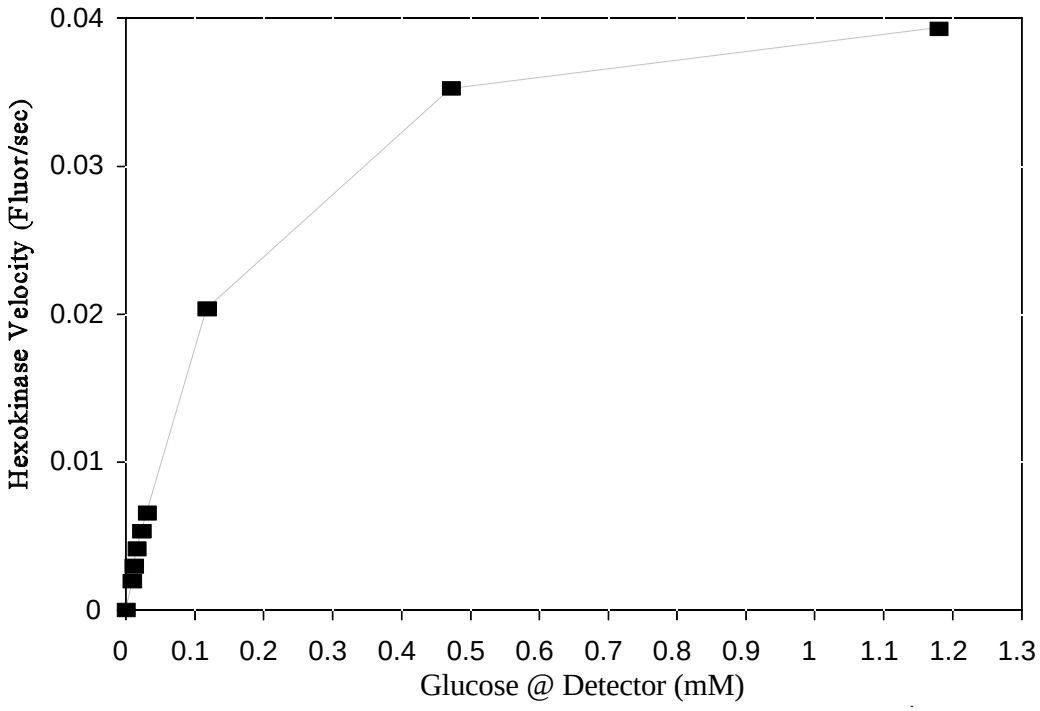

Figure 3.14. Large ByT-FAS system generated Michaelis-Menten plot of hexokinase velocity as a function of glucose concentration.

Glucose concentrations at the point of detection assayed were 0, 0.005, 0.011, 0.016, 0.023, 0.031, 0.112, 0.472, and 1.12 mM. $NADP^+$ and ATP were 5 mM at the point of detection in all assays for glucose. The ratio of hexokinase to coupling enzyme was 1/3.5 at the point of detection.

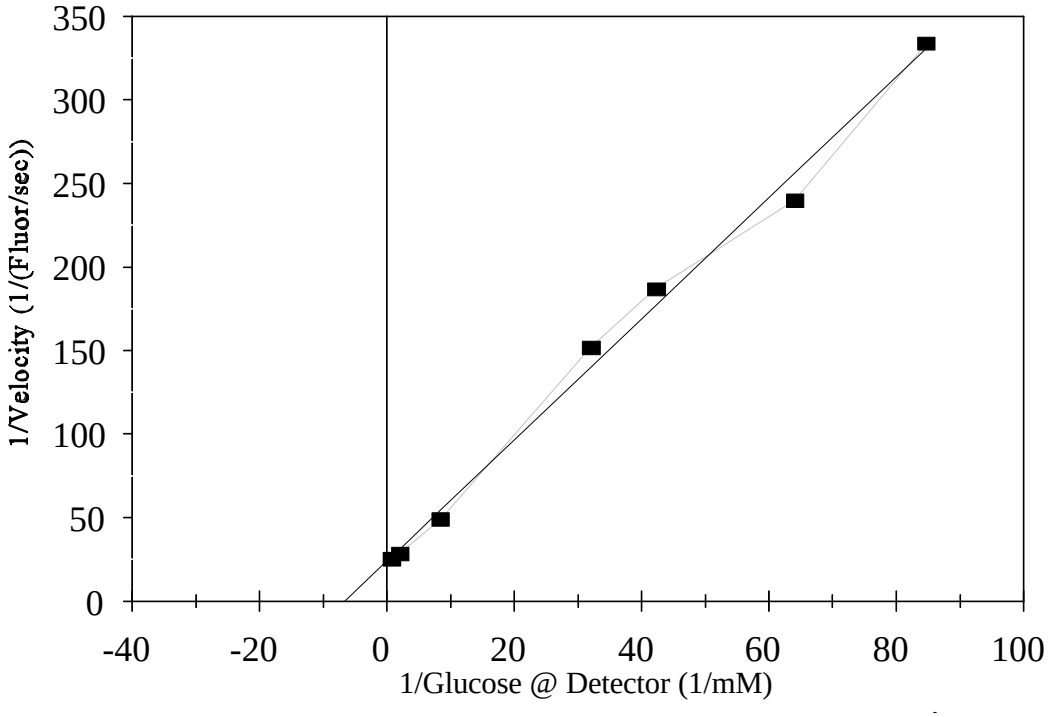

Figure 3.15. Large ByT-FAS system generated Lineweaver-Burk plot of hexokinase velocity as a function of glucose concentration.

The Km of glucose with hexokinase calculated as the negative reciprocal of the x-intercept (-1/Km).
— Regression line.

1.10 Hexokinase Velocity as a Function of ATP Concentration in the Presence of Competitive Inhibitor ADP

The Lineweaver-Burk plot of hexokinase velocity as a function of ATP concentration at different levels of ADP is shown in Figure 3.16. As shown in Table 3.4, both the Km for ATP and the Ki for ADP compare well with literature values for the two constants. This validates the capability of ByT-FAS to perform more complex biochemical measurements and generate accurate results.

Table 3.4 Comparison of ByT-FAS versus Literature Values for Some Kinetic Constants of Yeast Hexokinase

	ByT-FAS	Literature Value[47]
ATP-Km (*u*M)	269 ± 20	200
ADP-Ki (mM)	1.2 ± 0.1	1.14

Small ByT-FAS Design

2.1 Additivity of Fluorescence Investigation Using a Syringe Pump and Smaller Internal Diameter Tubing

Using a syringe pump with a reagent to sample carrier stream flow ratio of 2.5/1, an additivity of fluorescence was performed to investigate the consequences of a significant change in the ratio of flows on attaining physical steady state. Quinine was injected as the tracer for fluorometric detection. The reagent and sample streams merged at the cross in a head on manner and turned ninety degrees to flow towards the detector cell as shown in Figure 2.1 (Material and Methods). As can be seen in Figure 3.17, the quinine injected into the sample carrier stream appears to never achieve a constant physical steady state signal. However, the quinine injected into the reagent carrier stream does appear to reach a constant physical steady state signal. Also, the separate reagent and sample injection traces add up to more

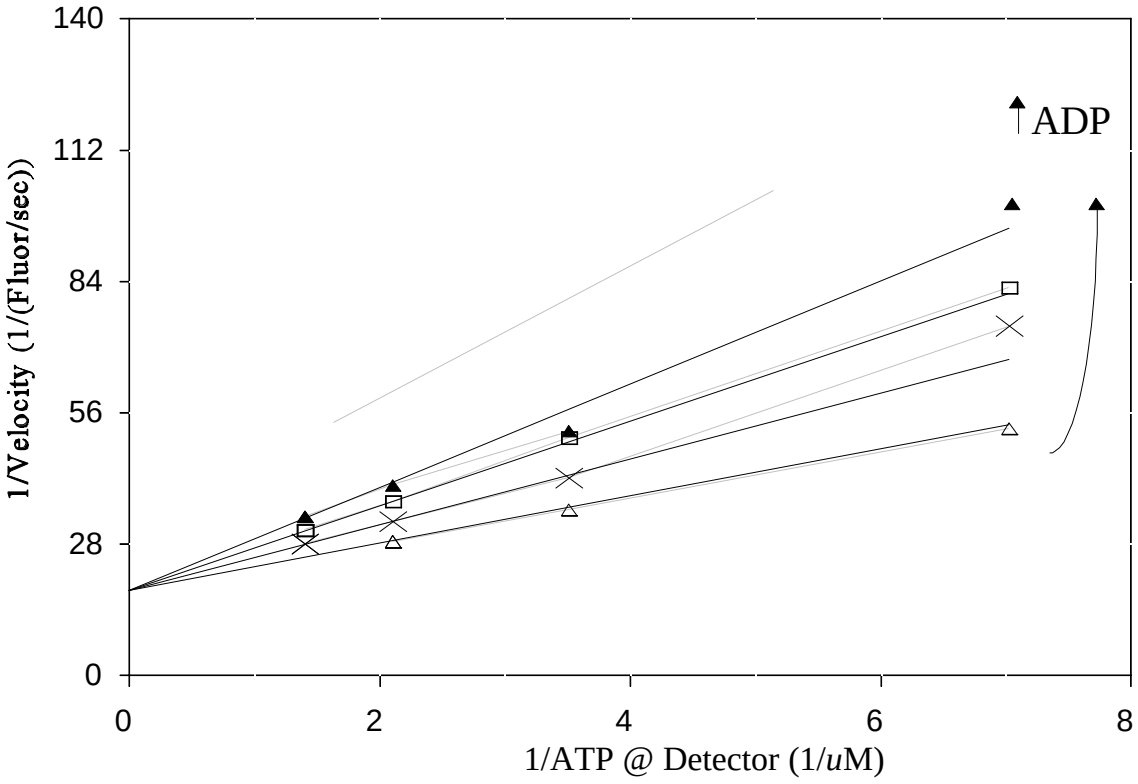

Figure 3.16. Large ByT-FAS system generated Lineweaver-Burk plot of ADP inhibition of ATP with hexokinase.

Large ByT-FAS system determinations of the Km for ATP with hexokinase and the Ki for ADP on ATP. Δ- No ADP, × - 0.47 mM ADP, □ - 0.95 mM ADP, ▲ - 1.42 mM ADP. $NADP^+$and glucose were 5 mM at the point of detection in all assays. — Regression lines.

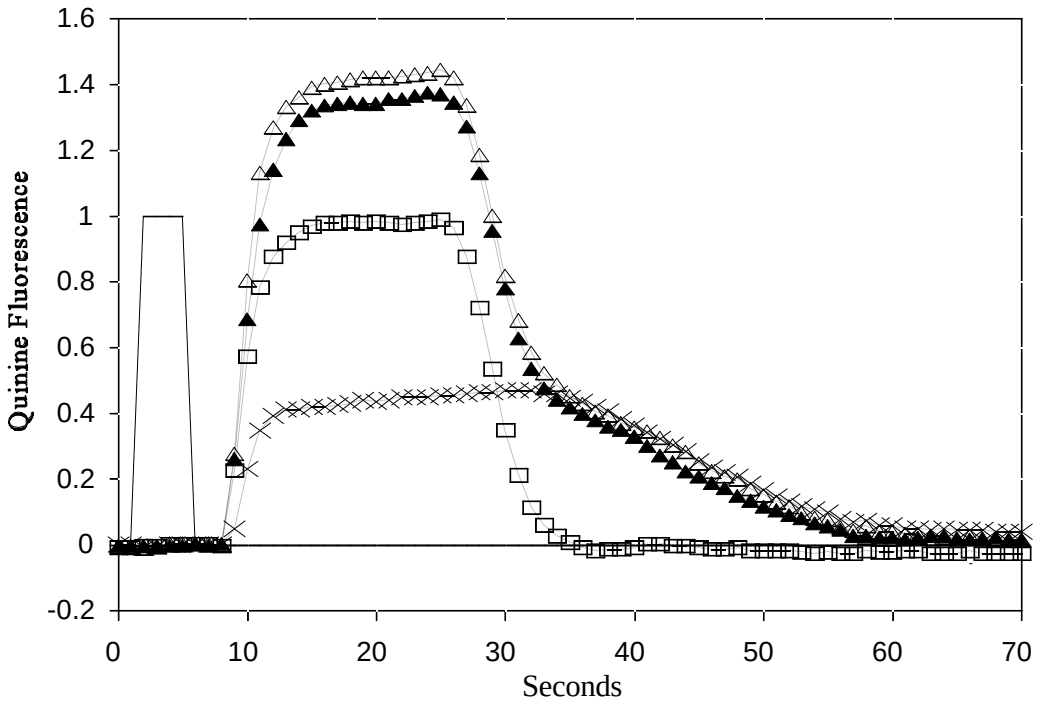

Figure 3.17. Syringe pump test for additivity of fluorescence with head on merging in ByT-FAS cross.

Reagent to sample carrier stream flow ratio of 2.5/1 (25 mL to 10 mL Syringes). Reagent and sample carrier flow streams merging head on in the cross (See Figure 2.1). × - quinine injected into sample carrier stream only, □ - quinine injected into reagent carrier stream only, ▲ - quinine injected into reagent and sample carrier streams simultaneously, Δ- Sum of quinine sample (×) and reagent (□) carrier stream traces added together. Sample and reagent injected quinine traces do not display an additivity of fluorescence compared to the injection of quinine into both simultaneously.

than the signal from the simultaneous injection indicating a non-laminar flow pattern. Because the flow rate of the reagent stream is 2.5 times greater than the sample stream, and the streams merge head on in the cross, a sample may not retain its bolus integrity after merging with the reagent stream. From the data in Figure 3.17, it appears that the sample bolus never achieves a steady detector signal, instead it continuously rises. It was postulated that changing the merging angle of the reagent and sample streams in the cross from head on to ninety degrees will enable the sample to achieve a steady detector signal.

2.2 Additivity of Fluorescence, Effects of Angle of Convergence at the Cross

To examine the effect of the angle of convergence in the cross, the ByT-FAS system flow schematic was changed to that in Figure 2.2 (Material and Methods) to allow the larger reagent stream flow rate a direct path to the detector cell. As shown in the flow schematic in Figure 2.2, the sample carrier stream meets the reagent stream at a ninety degree angle. This flow schematic allows the sample bolus to enter the faster reagent flow stream less disruptively.

Shown in Figure 3.18 is the additivity of fluorescence experiment using the ByT-FAS flow schematic shown in Figure 2.2. As can be seen, the quinine injected into both the sample and reagent carrier streams appear to attain a constant physical steady state signal. Also, the separate reagent and sample injection traces add up to the simultaneous injection trace. The only flow system difference between this data and that in Figure 3.17 is the orientation of convergence of the streams at the cross. As a result of the differences shown between Figures 3.17 and 3.18, when the reagent and sample carrier stream flow rates are not equally matched, a ninety degree angle of convergence at the cross should be employed.

2.3 Investigation of a 5 *u*L Fluorescent Tracer to Reach Physical Steady State

Using a syringe pump to facilitate a reagent to sample carrier stream flow ratio of 10/1, a quadruplicate injection of five microliters of a quinine tracer was made into the sample side

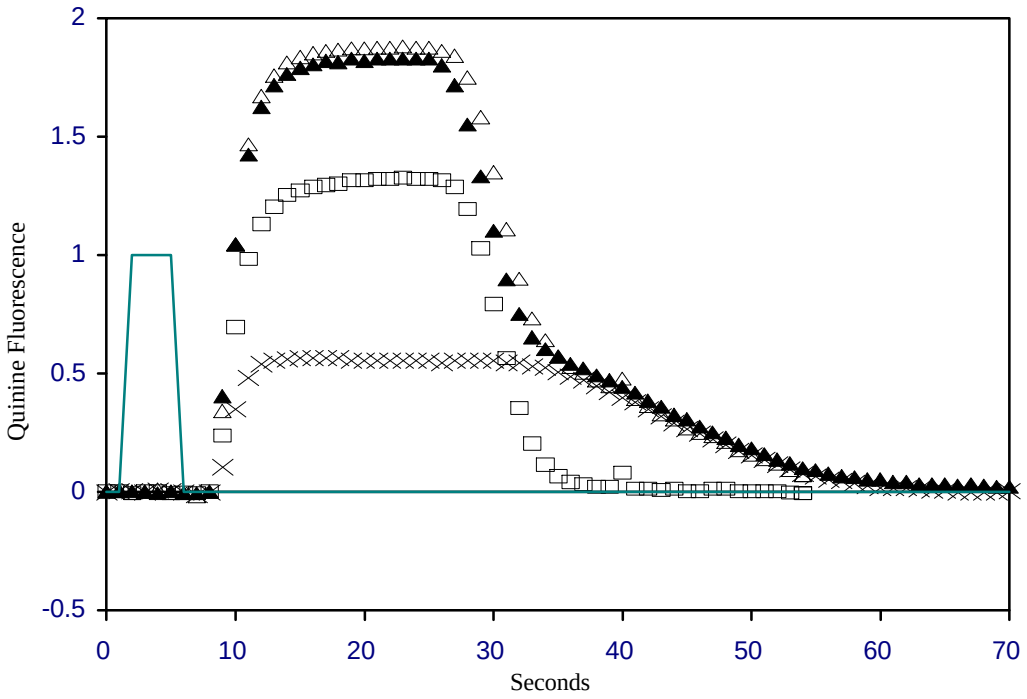

Figure 3.18. Syringe pump test for additivity of fluorescence with ninety degree angle of merging in ByT-FAS cross.

Reagent carrier flow to sample carrier flow ratio of 2.5/1 (25 mL to 10 mL Syringes). Reagent and sample carrier flow rates merging at a 90° angle in the ByT-FAS cross (See Figure 2.2). ✕ - quinine injected into sample carrier stream only, □ - quinine injected into reagent carrier stream only, ▲ - quinine injected into reagent and sample carrier streams simultaneously, Δ- Sum of quinine sample (✕) and reagent (□) carrier stream traces added together. Sample and reagent injected quinine traces display good additivity of fluorescence compared to the injection of quinine into both simultaneously. Quinine injected into the sample carrier stream has a very noticeable plateau of detector signal indicating smooth merging with the reagent carrier stream.

of the system to visually determine the attainment of physical steady state. The five microliter injections were made at two different total system flow rates. The raw data traces of the injections are shown in Figure 3.19. From Figure 3.19 it may appear that the 5 *u*L injections attained physical steady state for three seconds at the 0.22 mL/min flow rate and five seconds at the 0.11 mL/min flow rate. However, when an actual assay system was used based on this appearance, the data did not correspond to absolute manual measurements. As a result, visual inspection of physical steady state attainment does not appear to be reliable or accurate.

2.4 Additivity of Fluorescence for 5 *u*L Sample Volume and 70 *u*L Reagent Volume

Using a syringe pump to facilitate a reagent to sample carrier stream flow ratio of 10/1, an additivity of fluorescence was performed to demonstrate the overlap of 5 *u*L sample injections and 70 *u*L reagent injections at physical steady state. As can be seen in Figure 3.20, the quinine injected into the sample carrier stream appears to have achieved a constant physical steady state signal for about five seconds. The quinine injected into the reagent stream appears to have attained a constant physical steady state signal for about ten seconds. Together, the signals appear to overlap for about five seconds between 32 - 37 seconds of the ByT-FAS run. This apparent visual overlap of physical steady state signals is a subjective interpretation of the analyst. A more rigorous determination of when physical steady state is achieved and for how long needed to be developed.

2.5 Sample Physical Steady State Validation With Absolute Measurement

To unequivocally define when physical steady state is achieved for an injected analyte, the absolute signal for the analyte to be injected must be determined. Shown in Figure 3.21 is the absolute fluorescence signal expressed as a percentage of the average detector signal of the quinine tracer between 40 and 120 seconds in the run. The quinine tracer was at complete saturation in the sample carrier flow stream. Also shown are quadruplicate 25 *u*L injections of the same quinine tracer solution for their ability to reach the same fluorescence signal.

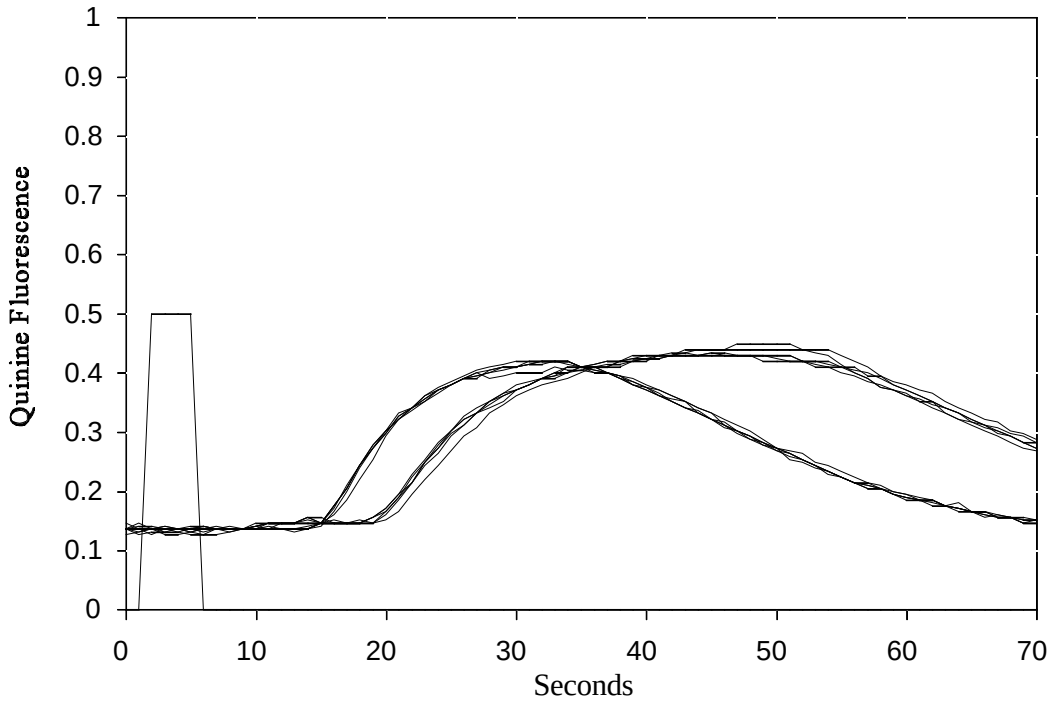

Figure 3.19. Small ByT-FAS system 5 uL quinine tracer injected into sample carrier stream.

Reagent to sample carrier stream flow ratio of 10/1. Quadruplicate injections of five microliters of injected quinine tracer for visible qualitative determination of physical steady state attainment. Total system flow rate for first set of quinine peaks is 0.22 mL/min. Total system flow rate for seconds set of quinine peaks is 0.11 mL/min. Qualitatively, the quinine injections visually appear to plateau and reach physical steady state for a few seconds.

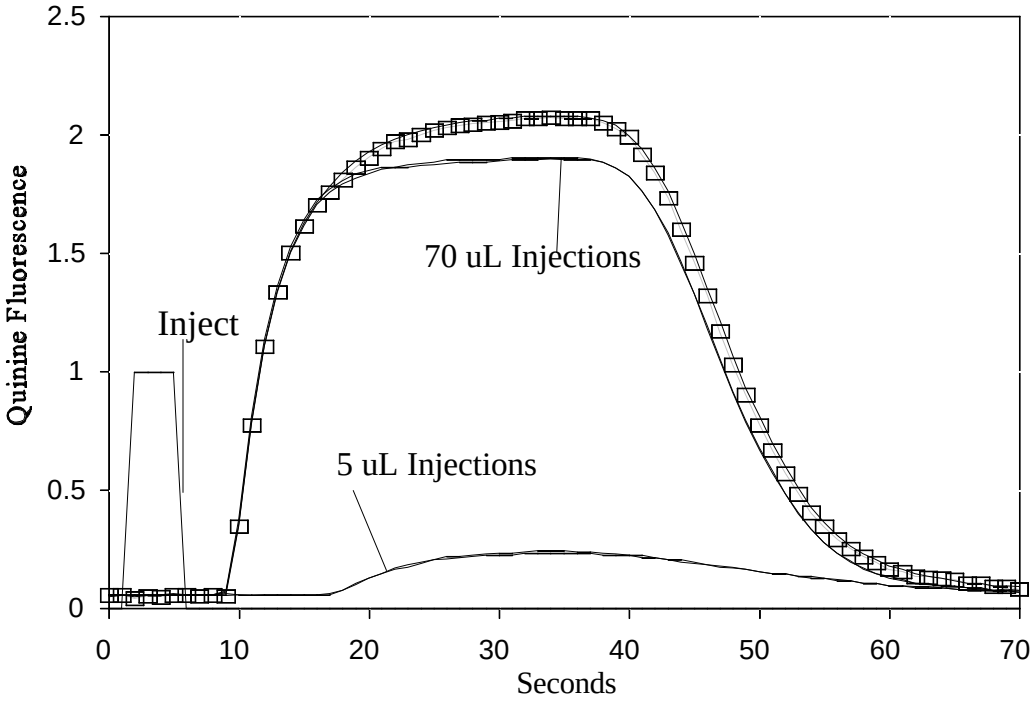

Figure 3.20. Small ByT-FAS system additivity of fluorescence for reagent and sample carrier flow ratio of 10/1.

Apparent overlap of reagent and sample carrier flow streams at physical steady state. Sample carrier stream 5 *u*L quinine injection, and reagent carrier stream 70 *u*L of quinine.
— - reagent and sample carrier stream quinine traces injected simultaneously. □ -Sum of reagent (70 *u*L) and sample (5 *u*L) carrier stream traces added together

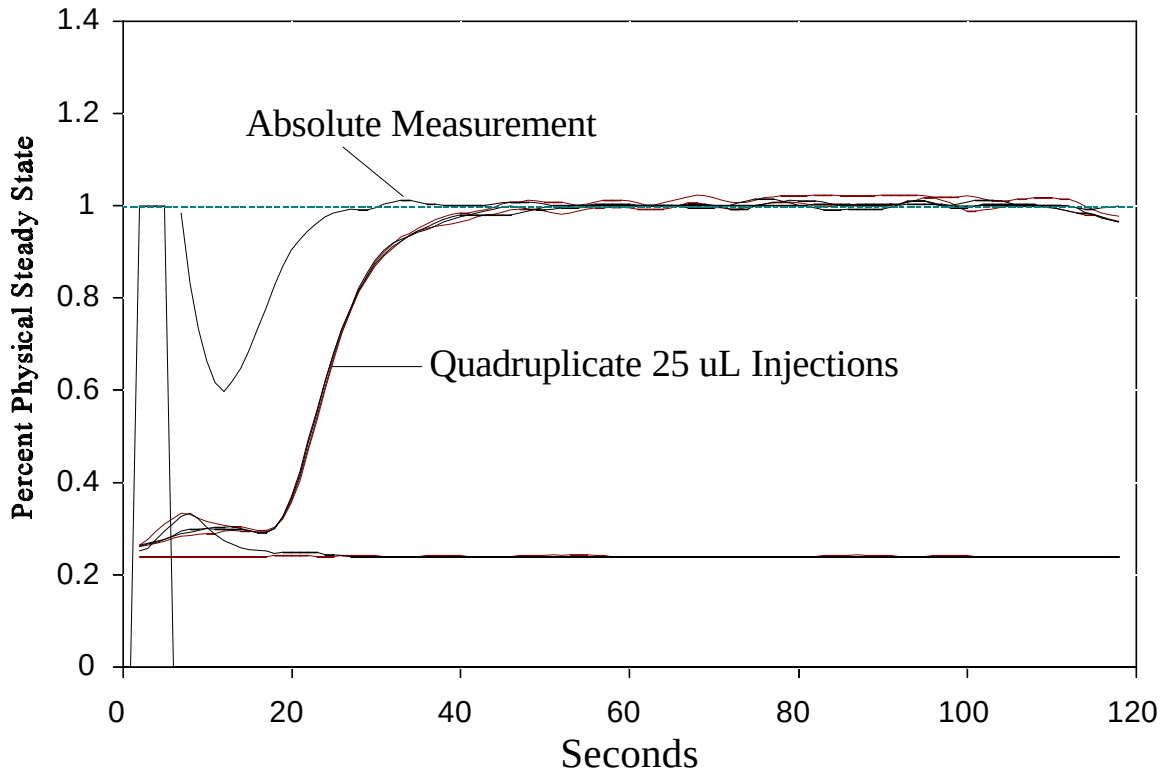

Figure 3.21 Small ByT-FAS system calibration of physical steady state with an absolute measurement.

Quinine was loaded into the sample syringe reservoir to saturate the sample carrier stream side of ByT-FAS and the detector cell with an absolute measurement of quinine tracer. The system was then flushed and run with multiple 25 *u*L injections of the same tracer solution to determine when physical steady state is reached. Reagent to sample carrier stream flow ratio of 10/1 (25/2.5 mL syringes). Total system flow rate of 0.22 mL/min.

Clearly, the 25 *u*l injections did reach physical steady state concentrations in the detector cell at approximately 42 seconds into the run and stayed there for over a minute.

Shown in Figure 3.22 is a Y - axis expansion between 95 - 105% of the data shown in Figure 3.21. Also shown in Figure 3.22 are the 1σ, 2σ, and 3σ bars around the average absolute fluorescence signal. From this graph, it can be seen that the quinine traces vary around the absolute measurement by 1 - 2%. This could be a result of slight pulsations in the flow rate delivered from the syringe pump or detector noise, perhaps both. Regardless, it is evident that the 25 *u*L injections do reach and sustain physical steady state between 45 and 110 seconds in the ByT-FAS run.

Because the absolute measurement in ByT-FAS is too tedious for routine analysis of different configurations, a statistical definition for the attainment of physical steady state without performing an absolute measurement is described below.

Using a triplicate injection of a sample that reaches a reproducible maximum signal for a minimum of 20 seconds, determine the approximate time interval that physical steady state is achieved. Using this time interval, calculate the average physical steady state signal for all raw data traces and define that average signal as the value for 100% physical steady state. Convert the raw data traces to percent of physical steady state by dividing each signal data point by the average signal at physical steady state. Smooth out the percent of physical steady state data by making a moving box-car average of the data in the form of (00X00). Determine the standard deviation of the data over the same time interval as the average physical steady state signal described above. Average the standard deviations calculated from each set of smoothed data. Determine the percentage value of -1σ, -2σ, -3σ, and +1σ, +2σ, +3σ standard deviations away from 100% physical steady state.

When a sample signal enters the zone above -2σ standard deviations away from 100% physical steady state, it cannot be statistically excluded from having reached physical steady state. As long as the signal varies between -3σ and +3σ standard deviations of the 100% signal, without a noticeable trend, the sample bolus can be considered at physical steady state.

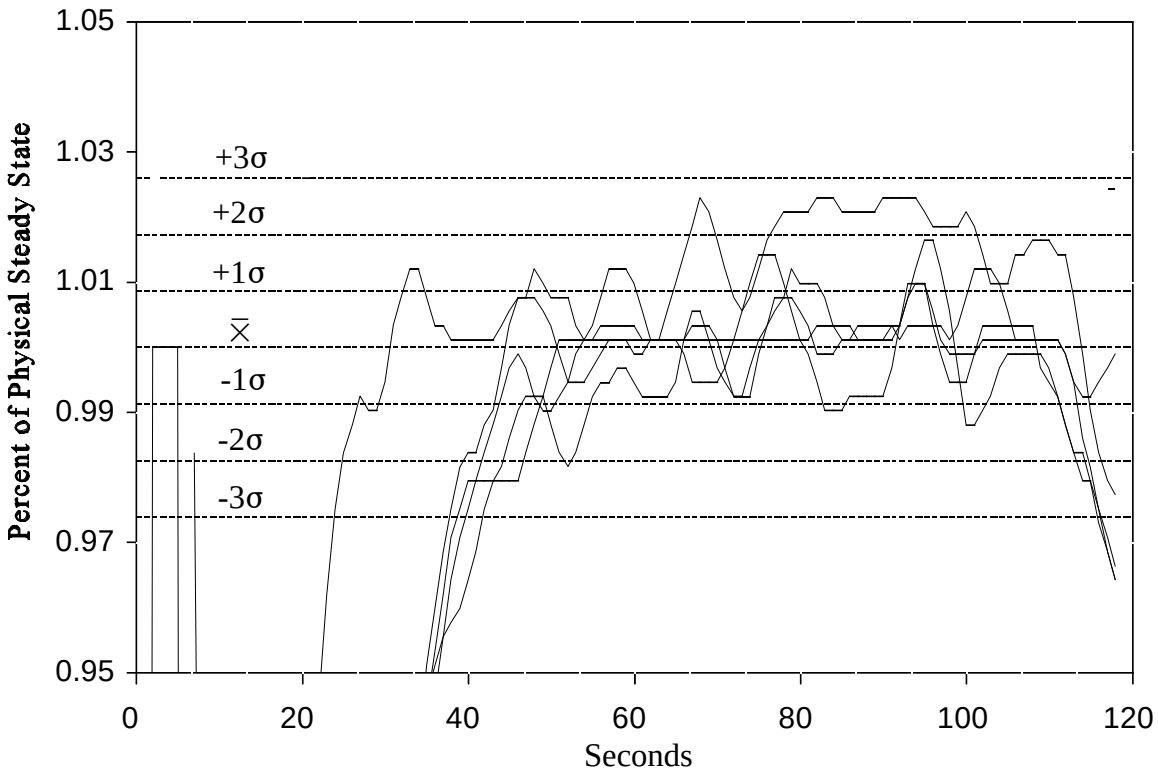

Figure 3.22. Y-axis Expansion of Figure 3.21.

For calculation of first, second, and third standard deviation lines of raw data around 100 percent physical steady state see text. Absolute measurement graphed with quadruplicate injections of a 25 *u*L quinine tracer. Reagent to sample carrier stream flow ratio of 10/1 (25/2.5 mL syringes). Total system flow rate of 0.22 mL/min.

2.6 Low Molecular Weight Analyte; Effects of Sample Volume on Reaching Physical Steady State With 0.0025" Sample Side Tubing Internal Diameter

Shown in Figure 3.23 are fluorescence quinine traces in quadruplicate from injected volumes of 5, 10, 15, and 25 *u*L into the sample carrier flow stream. The reagent to sample carrier stream flow ratio was 10/1. Shown in Figure 3.24 are the same data expressed as a percentage of physical steady state as calculated from the average signal of the 25 *u*L injections between 50 and 110 seconds of the run. From this data, the time interval that each injected volume attains a physical steady state signal can be tabulated. Shown in Table 3.5 are the time intervals that each volume injection shown in Figure 3.24 was calculated to be at physical steady state.

Table 3.5 Seconds of run that sample reaches physical steady state for a 10/1 flow ratio and 0.0025" sample side tubing internal diameter.

	Injected Volumes			
Run	5 *u*L	10 *u*L	15 *u*L	25 *u*L
1	0 s	37 - 54 s	37 - 79 s	41 - 119 s
2	0 s	37 - 55 s	37 - 77 s	40 - 112 s
3	0 s	38 - 56 s	36 - 77 s	40 - 113 s
4	34 - 35 s	37 - 55 s	37 - 77 s	39 - 110 s

From this data, it is apparent that the 5 *u*L injections do not attain a physical steady state signal reproducibly. This data compared to the data from experiments 2.3 and 2.4 illustrates why a visible inspection of physical steady state is not reliable or accurate. Also shown in Table 3.5 is the time difference for achievement of physical steady state between the 15 *u*L and 25 *u*L injections. The 25 *u*L sample loop is two-thirds longer than the 15 *u*L sample loop.